RESEARCH ARTICLE

A Dimension-Independent Array Relocation (DIAR) Approach for Partial Shading Losses Minimization in Asymmetrical Photovoltaic Arrays

PRADYUMNA MALLICK [1]**, RENU SHARMA** [1]**, (Senior Member, IEEE),**
PRIYA RANJAN SATPATHY [2]**, SUDHAKAR BABU THANIKANTI** [2,3]**, (Senior Member, IEEE),**
AND NNAMDI I. NWULU [3]**, (Senior Member, IEEE)**

[1]Department of Electrical Engineering, ITER, Siksha 'O' Anusandhan Deemed to be University, Bhubaneswar 751030, India
[2]Department of Electrical and Electronics Engineering, Chaitanya Bharathi Institute of Technology, Hyderabad 500075, India
[3]Centre for Cyber Physical Food, Energy and Water Systems, University of Johannesburg, Johannesburg 2006, South Africa

Corresponding author: Sudhakar Babu Thanikanti (sudhakarbabu66@gmail.com)

ABSTRACT Solar photovoltaic (PV) power system consists of numerous modules connected in series and parallel to generate a certain range of voltage and current outputs. However, the modules are highly vulnerable to the frequently occurring scenario of partial shading that results in severe losses of power, hotspot, system performance reduction, and permanent damage to the modules. These problems are mainly diminished through reconfiguration strategies that disperse the intensity of shading among the modules to reduce current mismatch and increase the power output of the system. But the pre-existing reconfiguration techniques exhibit one major demerit toward the limited application in symmetrical or square arrays that are quite uncommon in the real-time scenario. Hence, this paper presents a Dimension-Independent Array Relocation (DIAR) approach for the modules connected to asymmetrical arrays that enhance the output power of the system during all patterns of partial shading scenarios. The methodology is simple, easy to implement, cost-effective, and a one-time arrangement for the modules of the system that ensures lower power losses and higher reliability during partial shading. The methodology has been tested for 6×3, 5×7, 20×4, and 4×3 (experimental analysis) asymmetrical arrays and compared with conventional connections under numerous partial shading cases in the MATLAB/Simulink environment. Additionally, the application of the proposed methodology to symmetrical arrays has been validated under partial shading and compared to three pre-existing reconfiguration strategies. From the depth investigation, the average efficiency of power conversion has been noted as 98.04% with an average power enhancement of 18.34% than conventional techniques.

INDEX TERMS Efficiency, hotspot, mismatch loss, partial shading, power loss, reconfiguration.

I. INTRODUCTION

Photovoltaic (PV) is the most preferred energy generation source that plays an important role in the development of global energy scenario [1]. The wide source availability, eco-friendly, noiseless generation, and area independence

installation are some of the major merits that attracted a wide audience to opt for the solar PV system. However, the PV system faces one major challenge i.e., operation under non-uniform irradiance that affects the power generation, characteristics, performance, and reliability the most [2]. The non-uniform irradiance occurs when the modules operate under partial shading that is caused due to shadow of nearby objects such as buildings and trees, cracked glass, dust

coverage, and clouds (in the case of large power plants) [3]. This causes multi-power peaks in the power characteristics curves of the system leading to false tracking operation of the maximum power point tracking (MPPT) algorithms creating complications and further losses [4]. Also, the modules under shading are highly susceptible to physical damage caused by hotspot as it acts as a load and consumes current as compared to other normal operating modules that generate higher current [5]. A study on the effect of partial shading in long strings and parallel strings is done that suggested reducing the connection of long strings and parallel strings through a single inverter to the electrical grid to reduce shading losses [6]. Various connection methodologies have been proposed for PV modules such as series-parallel (SP), total-cross-tied (TCT), honeycomb (HC), and bridge-linked (BL) to boost power generation during partial shading [7]. Most of the studies have claimed the TCT topology to be effective with higher power-generating capability during partial shading [8]. Also, these topologies have been tested with and without the presence of bypass diodes in the PV modules with the conclusion as the power losses during partial shading depend on the irradiance level and pattern of shading [9]. Also, another study compared these topologies in terms of power generation and fill factor under partial shading with the outcome as TCT having notably higher performance [10]. In addition, implementation of TCT requires no extra cost however, the optimal dispersion of shade is not possible and power generation can be further enhanced than TCT.

Later on, an electrical array reconfiguration (EAR) has been proposed to disperse the partial shading in PV arrays by changing the electrical connection of modules through a fast-switching matrix [11]. Two different methodologies based on the fuzzy-logic controller (FLC) [12] and neuro-fuzzy interference (NFI) [13] have been proposed to enhance the maximum power point of the power curves during partial shading. Also, a rough set theory has been proposed that dynamically reconfigures the TCT, BL, HC, and SP during partial shading [14]. An algorithm on Munkres optimization based on the irradiance equalization technique has been proposed with increased processing speed for finding the optimal reconfiguration of modules during non-uniform irradiance [15]. Similarly, another current variation index (CVI) based technique named as scanning technique has been proposed that uses the row current algorithm to estimate the best reconfiguration for modules during partial shading [16]. A switching matrix with less computational time and iteration counts based on dynamic reconfiguration i.e., greedy algorithm controller has been proposed to dynamically reconfigure the connection of the module for proper shade dispersion and higher power generation during partial shading [17]. However, the major demerits of the EAR technique include the requirement of a monitoring system, multiple switching patterns, and sensor count that increase the overall cost and complexity of the system.

Hence, to overcome the demerit of the EAR, various optimization-based reconfiguration techniques such as genetic algorithm (GA) [18], particle swarm optimization (PSO) [19], grasshopper algorithm (GOA) [20], dragonfly algorithm [21] and many more have been proposed. These algorithms are simple and find the optimal connection in less time with reduced switch counts. Two algorithms based on Harris Hawks Optimization (HHO) and modified Harris Hawks Optimization (MHHO) have been proposed and tested for 9×9 and 6×20 arrays, compared with TCT, GA, and PSO where MHHO found to be effective in dispersing the shading with higher computational speed and reduced iteration [22]. Similarly, another reconfiguration based on grey wolf optimization (GWO) has been proposed for series and series-parallel connections with lower controlling parameters and higher power generation than PSO during partial shading [23]. Similarly, an easy-to-implement and higher shade dispersion capability reconfiguration-based butterfly optimization algorithm (BOA) has been proposed with better performance than SP, TCT, and GWO under shading [24]. These optimizations-based dynamic reconfiguration techniques enhance the power generation of the array with reduced computational time and switch counts but, still, the major demerit lies in the practical implementation and most of these techniques are tested for 9×9 symmetric arrays.

Hence, considering the practical, easy, and cost-effective implementation in PV arrays, static reconfigurations have gained an enormous audience to reduce shading losses. The static reconfiguration changes the positions of the modules physically for one-time to disperse the shading in the array [25]. The most popular technique of static reconfiguration is the Sudoku puzzle which effectively disperses the shading but, the major demerit lies in the long wires' requirement and dedicated application to a 9×9 array [26]. However, the long wires requirement demerit of the Sudoku technique has been solved through the proposal of optimal Sudoku [27] and improved Sudoku [28] techniques but, they still get limited to 9×9 arrays. Later on, an Arrow-Sudoku technique has been proposed and tested for a 6×6 array and found to generate higher power than TCT, SP, HC, BL, TCT-SP, HC-TCT, and BL-TCT during partial shading [29]. However, to overcome the limitation of wire length in the Arrow-Sudoku technique, a new skyscraper reconfiguration is proposed with higher power generation during partial shading [30]. A magic square (MS) reconfiguration has been proposed and found to be the most suitable technique for enhancing the power output of the TCT connection during partial shading [31]. Similarly, two other MS reconfiguration techniques have been proposed in [32] and [33] and tested for 4×4 and 6×6 arrays respectively with results showing higher power generation during partial shading. A novel MS technique for the rearrangement of modules for shade dispersion has been proposed that generated higher energy during partial shading than TCT and Sudoku techniques under long and

wide shading [34]. An odd-even reconfiguration has been proposed that disperses the shading to enhance the power generation of the array more than the TCT configuration [35]. Another two-phase array reconfiguration has been proposed and tested for 9×9 and 18×18 TCT arrays that generated higher power and efficiency than the TCT, Sudoku, and PSO but, the complex wiring structure can increase the power loss, complexity, and cost of the system [36]. Similarly, various other static reconfiguration techniques have been proposed such as image encryption [37], Shade Dispersion Scheme (SDS) [38], Fixed Electrical Reconfiguration (FER) [39], Henon map [40], and many more have been proposed for shade dispersion to increase the power output of the PV arrays during partial shading. These techniques are cost-effective and easy to implement in PV arrays with higher power generation during partial shading but, the major demerit lies in the limited application to square/ symmetric arrays.

Hence, to overcome the limitations such as requirements of sensors and switches, limited application to the square or symmetrical PV arrays sizes and practical implementation, the following works has been conducted in this paper:

➢ A Dimension-Independent Array Relocation (DIAR) approach for PV arrays is proposed.

➢ DIAR disperses the partial shading in the array to reduce the current mismatch by relocating the modules for one time.

➢ Applicable for asymmetrical and symmetrical sizes of PV arrays.

➢ DIAR utilizes a simple and easy to understand methodology for relocation.

➢ No requirements of any switches, sensors or additional components for operation.

➢ Cost-effective and easy to implement.

➢ DIAR is tested for four asymmetrical i.e., 6×3, 5×7, 20×4, and 4×3 along with 7×7 symmetrical PV arrays.

➢ Performance of the DIAR is compared with the total-cross-tied, honeycomb, series-parallel and bridge-linked configurations along with three existing reconfigurations.

➢ Validated using the MATLAB simulation and prototype experimental setup platforms under realistic partial shading scenarios.

II. SYSTEM DESCRIPTION

The PV modules are the major component of the arrays that are modeled in MATLAB/Simulink using the equation given below.

$$I_O = I_P - I_D[exp((V_M + (R_S * I_M))/I) - 1] - [(V_M + (I_M * R_S))/R_{Sh}] \quad (1)$$

'I_O', 'I_P', 'I_D', 'V_M', 'R_S', 'I', and 'R_{Sh}' are the module current, photo-current, diode current, voltage, series resistance, ideality factor, and shunt resistance respectively. The rating of the modules used for the MATLAB/Simulink modeling is 325W (maximum power), 37.80V (maximum
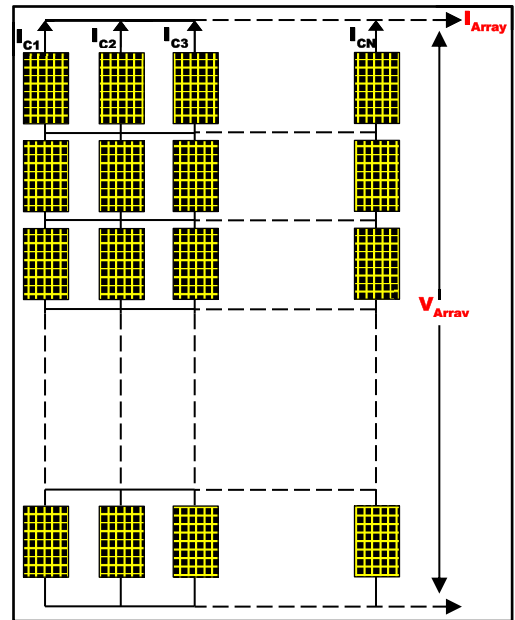

FIGURE 1. PV array of MxN dimension with TCT connection.

voltage), 8.60A (maximum current), 46.40V (open-circuit voltage), and 9.20A (short-circuit current).

In total cross tied (TCT) connection, the modules of each row are linked in parallel through cross-ties and then each row is connected in series as shown in FIGURE 1. The current generated by each module directly depends on the receiving irradiance by its surface. Hence, the current output of each row (I_{Rm}) can be calculated as

$$I_{Rm} = \sum_{i=1}^{m} \left(\frac{Irradiance}{1000} \times I_{M(ij)} \right) \quad (2)$$

where I_M, i, and j indicate the current output of PV modules under normal operation, row number, and column number respectively.

The output voltage (V_{Array}) and current (I_{Array}) of the PV array with a TCT connection can be calculated using Kirchhoff's Voltage and Current Law as

$$V_{Array} = \sum_{i=1}^{m} V_{Mi} \quad (3)$$

$$I_{Array} = \sum_{j=1}^{n} \left(I_{ij} - I_{(i+1)j} \right) = 0,$$
$$j = 1, 2, 3, \ldots, m - 1 \quad (4)$$

where V_{Mi} indicates the voltage of the PV module at i[th] row.

In this study, the PV array has been tested under the real-time scenario of 800W/m^2 irradiance and 50°C module temperature i.e., normal operation. The power outputs of the 6×3, 5×7, 20×4, and 7×7 arrays under normal operation have been noted as 4.93kW, 9.08kW, 22.34kW, and 11.27kW respectively. The partial shading in the PV arrays has been applied by lowering the irradiance of the modules under shading with different values of 100W/m^2, 200W/m^2, 300W/m^2, 400W/m^2, 500W/m^2, 600W/m^2, 700W/m^2, etc. The power-voltage characteristics graph of the PV arrays has

been extracted by connecting a variable load to the output from which the maximum power can be recorded.

The power loss in the PV array has been calculated from the difference between the power output under normal conditions and partial shading condition (P_O) given by

$$Power\ Loss\ (PL) = P_{Normal} - P_O \quad (5)$$

The mismatch loss in the array is the difference between the available power in the array during partial shading (P_T) and power output under partial shading (P_O) as

$$Mismatch\ Loss\ (ML) = P_T - P_O \quad (6)$$

The power losses reduction (LR) by any technique (P_{Lt}) than the SP (P_{LSP}) has been calculated as

$$LR = [(PL_t - PL_{LSP})/PL_{LSP}] \times 100 \quad (7)$$

The conversion efficiency of any technique has been calculated as the percentile of the ratio between power output under partial shading (P_O) and available power (P_T) given as

$$Conversion\ Efficiency\ (CE) = \frac{P_O}{P_T} \times 100 \quad (8)$$

The power enhancement by any methodology (P_{Me}) than the conventional SP connection (P_{SP}) has been calculated as

$$Power\ Enhancement\ (PE) = \frac{P_{Me} - P_{SP}}{P_{SP}} \times 100 \quad (9)$$

The efficiency of the array has been calculated using equation (10) where 'A' and 'G' denotes the area of modules and receiving irradiance respectively.

$$Efficiency\ (Eff) = \frac{P_O}{G \times A} \times 100 \quad (10)$$

III. DIMENSION-INDEPENDENT ARRAY RELOCATION (DIAR) APPROACH

Dimension-Independent Array Relocation (DIAR) approach has been proposed to disperse the partial shading in the asymmetrical arrays to increase the power generation of the system. Also, the proposed methodology is applicable for square or symmetrical arrays where the row and column counts are the same. The proposed approach requires no switches and sensors for power enhancement and is a one-time rearrangement of the modules without altering the electrical connection of the array. The rearrangement of the modules can be proceeded using simple and easy calculation steps without the requirement of programmable algorithms. The steps involved in the mathematical calculation of the DIAR approach have been explained below.

Step 1: Initially obtain the rows (M) and column (N) counts of the PV array.

Step 2: For *j=1* (column number), keep the positions of the modules unaltered i.e., *ij (new) = ij (old)* where *i*=1,2,......,*M* (row number), and k=0.

Step 3: Calculate *k=Round (M/2).*

Step 4: Similarly, for *j=2* shift the modules to their k^{th} position i.e., *ij(new)=(k)j* where *i*=*k* and *k*<*M*.

Step 5: For *j=N* (column number), shift the PV modules to their $k+b^{th}$ position i.e., *ij(new) = (k=b)j* where *i=k+b*, *k+b*<*M* and *b* is the incremented value of *k*.

Step 6: The modules will be permanently shifted based on the above calculation for effective shade dispersion during partial shading.

For a proper understanding of the proposed methodology, the above steps have been explained for the 6 × 3 PV arrays with a graphical presentation in FIGURE 2 (a). The steps involved in the DIAR approach for a 6 × 3 PV array have been explained below.

Step 1: First the number of rows (M) and columns (N) have been obtained as 6 and 3 respectively.

Step 2: For *j=1* (column 1), the value of *k* has been set as 0 i.e., the PV modules have been kept at the same position.

Step 3: The value of k has been calculated as *k=Round (6/3)=3.*

Step 4: For *j=2* (column 2), the PV modules have been shifted to their respective 3rd positions i.e., 12, 22, 32, 42, 52, and 62 have been shifted to their new positions at 32, 42, 52, 62, 12 and 22 respectively.

Step 5: For *j=3* (column 3), the modules have been shifted to their $k+1^{th}$ i.e., 4th positions, and hence, the modules located at 13, 23, 33, 43, 53, and 63 have been shifted to their new positions at 43, 53, 63, 13, 23 and 33 respectively.

Step 6: Hence, the PV modules have been shifted according to the DIAR approach.

Similarly, the example of the implementation of the DIAR approach to 5 × 7 and 20 × 4 PV arrays have been pictorially represented in FIGURE 2 (b) and (c) respectively. It has to be noted that the electrical connection of the arrays remains the same as TCT hence, the ratings of the system remain the same as that of TCT, BL, and HC. Also, the additional wire length requirement and losses associated with the proposed approach are very low as compared to the losses that occur in the conventional connections during partial shading and hence can be ignored.

IV. PERFORMANCE EVALUATION UNDER PARTIAL SHADING

The DIAR approach has been tested with three asymmetrical arrays of sizes 6 × 3, 5 × 7, and 20 × 4 along with a symmetrical array of 7 × 7 and compared with TCT, SP, BL, HC, and other existing reconfiguration techniques such as shade dispersion scheme (SDS) [38], fixed electrical reconfiguration (FER) [39], henon map [40] and magic square [31] (for symmetric 7 × 7 array). Later on, an experimental investigation on a 4 × 3 array has been conducted for the DIAR and compared with the TCT, BL, and SP connections under partial shading.

A. 6 × 3 ASYMMETRICAL PV ARRAYS

The proposed DIAR approach has been tested for a 6 × 3 PV array under eight partial shading patterns and compared
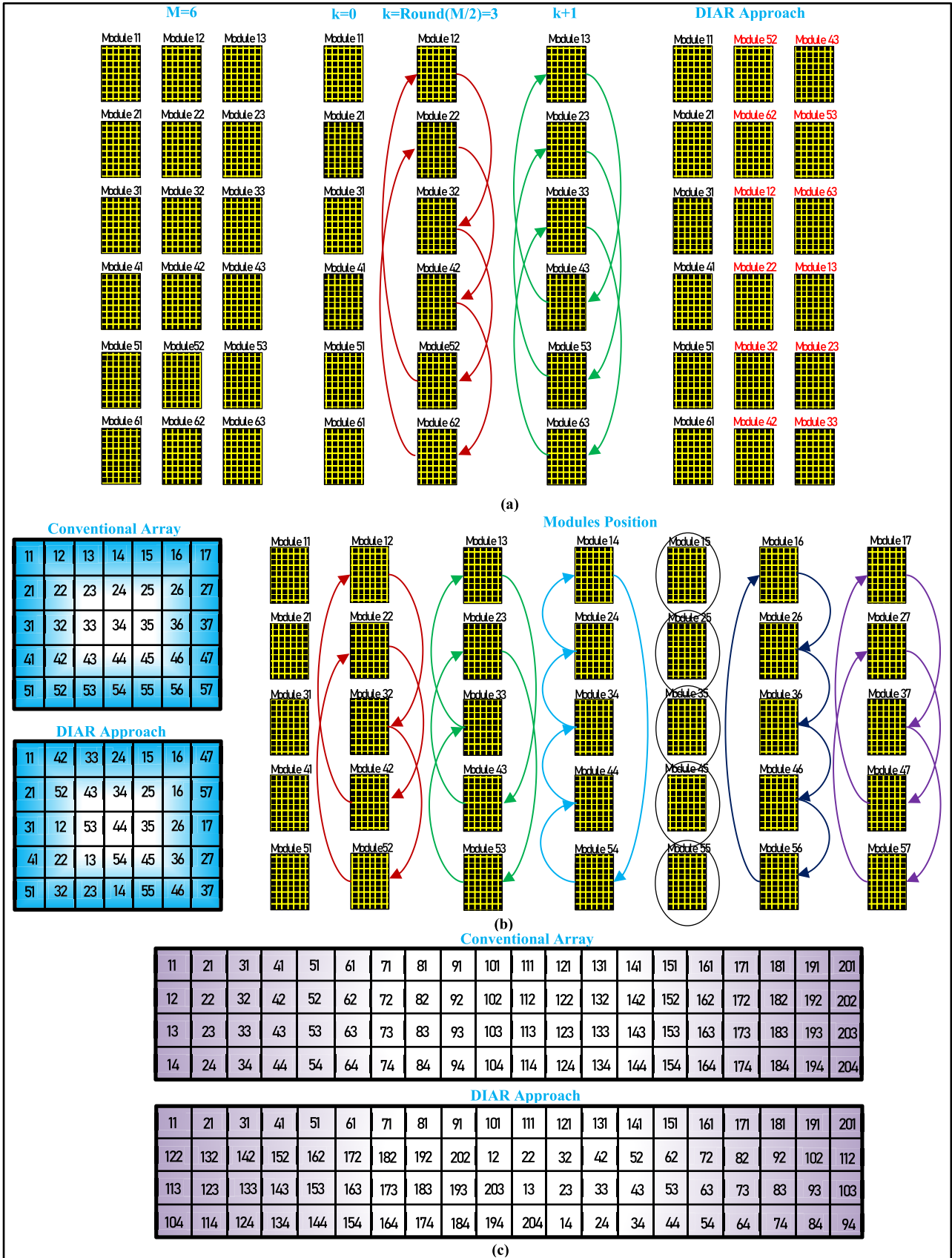
FIGURE 2. Implementation of the proposed DIAR approach in (a) 6 × 3, (b) 5 × 7, and (c) 20 × 4 asymmetrical PV arrays.

with the total cross tied (TCT) and series-parallel (SP) connections. The power output of the PV array under a normal operation scenario of 800 W/m^2 and 50°C has been recorded as 4.93kW.

1) PARTIAL SHADING PATTERN A1

The partial shading pattern for the 6×3 array has been shown in FIGURE 3 (a) where four modules of the array are receiving lower irradiance of 100W/m^2 and 200W/m^2. The irradiance under this situation by the TCT and SP has been shown in FIGURE 3 (b) and FIGURE 3 (c) shows the shade dispersion in the array through the DIAR approach. The power available in the array under this partial shading pattern has been calculated as 3.71kW.

The current output of the PV array with TCT connection for the first row has been calculated as

$$I_{(TCT)Row1} = \frac{100}{1000}I_M + \frac{200}{1000}I_M + \frac{800}{1000}I_M = 1.1I_M \tag{11}$$

where the current output of one module is represented by I_M.

Similarly, for other rows of the array, the current output has been calculated as

$$I_{(TCT)Row2} = \frac{100}{1000}I_M + \frac{200}{1000}I_M + \frac{800}{1000}I_M = 1.1I_M \tag{12}$$

$$I_{(TCT)Row3} = \frac{800}{1000}I_M + \frac{800}{1000}I_M + \frac{800}{1000}I_M = 2.4I_M \tag{13}$$

$$I_{(TCT)Row4} = \frac{800}{1000}I_M + \frac{800}{1000}I_M + \frac{800}{1000}I_M = 2.4I_M \tag{14}$$

$$I_{(TCT)Row5} = \frac{800}{1000}I_M + \frac{800}{1000}I_M + \frac{800}{1000}I_M = 2.4I_M \tag{15}$$

$$I_{(TCT)Row6} = \frac{800}{1000}I_M + \frac{800}{1000}I_M + \frac{800}{1000}I_M = 2.4I_M \tag{16}$$

Considering the presence of bypass diodes in the modules, the activation of the bypass diodes of the shaded modules allows the flow of $2.4I_M$ with a reduced voltage output of $4V_M+2V_D$ where V_D is the voltage of the bypass diode with $V_D <<< V_M$. However, the mathematical estimation of the array in activation of the bypass diodes is difficult and hence, the mathematical estimation has been done by considering the modules without bypassing. So, a total current output of $1.1I_M$ will flow through the PV array with a voltage output of $6V_M$. The power output of the array with a TCT connection without rows bypassing has been calculated as

$$P_{(TCT)} = 1.1I_M \times 6V_M = 6.6I_M V_M \tag{17}$$

Similarly, the current outputs from the rows of the PV array after dispersing the partial shading using the DIAR approach

(FIGURE 3 (c)) have been calculated below.

$$I_{(DIAR)Row1} = \frac{100}{1000}I_M + \frac{800}{1000}I_M + \frac{800}{1000}I_M = 1.7I_M \tag{18}$$

$$I_{(DIAR)Row2} = \frac{100}{1000}I_M + \frac{800}{1000}I_M + \frac{800}{1000}I_M = 1.7I_M \tag{19}$$

$$I_{(DIAR)Row3} = \frac{800}{1000}I_M + \frac{200}{1000}I_M + \frac{800}{1000}I_M = 1.8I_M \tag{20}$$

$$I_{(DIAR)Row4} = \frac{800}{1000}I_M + \frac{200}{1000}I_M + \frac{800}{1000}I_M = 1.8I_M \tag{21}$$

$$I_{(DIAR)Row5} = \frac{800}{1000}I_M + \frac{800}{1000}I_M + \frac{800}{1000}I_M = 2.4I_M \tag{22}$$

$$I_{(DIAR)Row6} = \frac{800}{1000}I_M + \frac{800}{1000}I_M + \frac{800}{1000}I_M = 2.4I_M \tag{23}$$

The current and voltage output of the PV array with the DIAR approach without bypassing the rows have been noted as $1.7I_M$ and $6V_M$. Hence, the power output of the array with the DIAR approach has been calculated as

$$P_{(DIAR)} = 1.7I_M \times 6V_M = 10.2I_M V_M \tag{24}$$

Hence, comparing the power outputs of the TCT and DIAR approach from equations (17) and (24), it can be found that the array with DIAR has generated higher power than TCT, and hence, the effectiveness of the shade dispersion by DIAR approach has been proved.

The power-voltage characteristics graph of the PV arrays with the TCT, SP, and DIAR approach for partial shading pattern 1 has been shown in FIGURE 3 (d). From the graph, it has been noticed that the DIAR has a notably higher power output of 3.69kW than the TCT (3.2kW) and SP (3.25kW). The power losses in the DIAR, TCT, and SP have been calculated as 1.24kW, 1.73kW, and 1.68kW whereas mismatch losses have been noted as 0.02 kW, 0.51kW, and 0.46kW respectively. The TCT and DIAR approach has -0.05kW and 0.44 kW loss reduction with -1.54% and 13.54% power enhancement than SP. The conversion efficiency and efficiency of the DIAR have been calculated as 99.46% and 15.11% which are higher than the SP (87.60% and 13.31%) and TCT (86.25% and 13.11%).

2) PARTIAL SHADING PATTERN A2

The partial shading pattern A2 has been shown in FIGURE 4 (a) where the first five modules of columns 1 and 2 are under lower irradiance of values as 100W/m^2, 200W/m^2, 300W/m^2, 400W/m^2, and 500W/m^2. The irradiance for TCT and SP has been given in FIGURE 4 (b) and the dispersion of shade by the DIAR approach has been shown in FIGURE 4 (c). The total available power in the PV array under this pattern has been calculated as 2.89kW. The current outputs of 1st row, 2nd row, 3rd row, 4th row, 5th row and
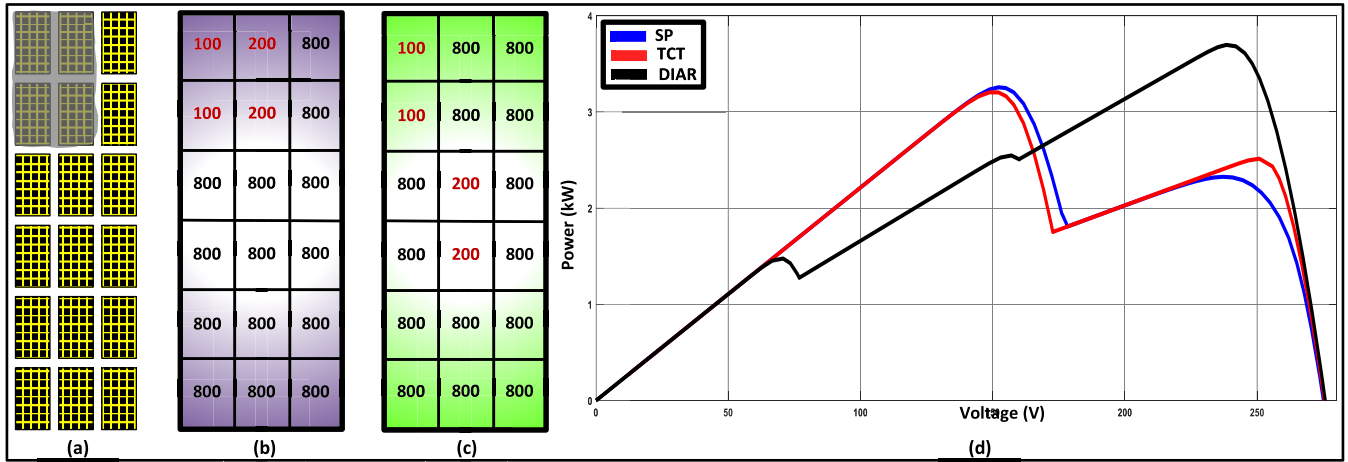
FIGURE 3. Partial shading pattern A1 for 6 × 3 PV array. (a) shading pattern, (b) irradiance in TCT and SP connection, (c) irradiance after shade dispersion by DIAR approach, and (d) power-voltage characteristics graph.

6th row have been estimated as $1I_M$, $1.2I_M$, $1.4I_M$, $1.6I_M$, $1.8I_M$ and $2.4I_M$ in TCT whereas $1.4I_M$, $1.8I_M$, $1.2I_M$, $1.4I_M$, $1.6I_M$ and $2I_M$ in DIAR respectively. Hence, the total power output from the TCT and DIAR has been mathematically estimated as $6I_M V_M$ and $7.2I_M V_M$ respectively.

The power-voltage graphs in FIGURE 4 (d) show the higher power generation capacity of the DIAR approach than the TCT and SP. The power generations of DIAR, TCT, and SP have been noted as 2.71kW, 2.29kW, and 2.31kW with 2.22kW, 2.64kW, and 2.62kW as power losses, 0.18kW, 0.6kW and 0.58kW as mismatch losses respectively. The TCT and DIAR have enhanced the power output of -0.87% and 17.32% than the SP respectively. The DIAR has the highest conversion efficiency of 93.77% than TCT (79.24%) and SP (79.93%). The efficiencies of the array have been calculated as 13.31%, 13.11%, and 15.11% for SP, TCT, and DIAR respectively.

3) PARTIAL SHADING PATTERN A3
During partial shading pattern A3, the bottom modules have been set under lower irradiance (FIGURE 5 (a)) with values as 500W/m^2 and 400W/m^2 as shown in FIGURE 5 (b). The row currents have been estimated as $2.4I_M$ (1st, 2nd, 3rd and 4th Rows), $1.5I_M$ (5th Row), and $1.2I_M$ (6th Row) for TCT and $2.1I_M$ (1st and 5th Rows), $1.7I_M$ (2nd Row), $2.0I_M$ (3rd and 6th Rows) and $2.4I_M$ (4th Row) for DIAR approach (FIGURE 5 (c)). The total power available in the PV array has been calculated as 3.80kW with mathematical power estimations as $7.2I_M V_M$ and $10.2I_M V_M$ for TCT and DIAR respectively. From the power-voltage graph given in FIGURE 5 (d), it can be observed that TCT and SP have equal power generation of 3.2kW but, the DIAR approach generated 3.79kW with 18.44% higher power than the TCT and SP. Also, the power and mismatch losses are minimum with values as 1.14kW and 0.01kW than TCT/SP with 1.73kW and 0.6kW respectively. The conversion efficiency of DIAR and TCT/ SP have been noted as 99.74% and 84.21% with efficiency as 15.52% (DIAR) and 13.11% (TCT/SP).

4) PARTIAL SHADING PATTERN A4
FIGURE 6 (a) shows the pattern of partial shading whereas the irradiance received by the TCT and SP with values as 600W/m^2, 500W/m^2, and 400W/m^2, and shade dispersion by DIAR have been shown in FIGURE 6 (b) and (c) respectively. The current generated by the 1st Row, 2nd Row, 3rd Row, 4th Row, 5th Row and 6th Row in the TCT have been calculated as $2.4I_M$, $2.0I_M$, $1.7I_M$, $1.5I_M$, $1.7I_M$ and $2.4I_M$ whereas for DIAR, $1.7I_M$, $2.0I_M$, $2.0I_M$, $2.2I_M$, $2.1I_M$ and $1.7I_M$ respectively.

So, the total power outputs of the PV array for this partial shading have been estimated as $9I_M V_M$ (TCT) and $10.2I_M V_M$ (DIAR). The power-voltage characteristics graph in FIGURE 6 (d) shows the power outputs where the DIAR, TCT, and SP have generated 3.68kW, 3.38kW, and 3.31kW from the total available power of 3.75kW. This states that the DIAR has the lowest mismatch loss of 0.07kW than TCT (0.37kW) and SP (0.44kW). The power loss in the DIAR approach gets reduced to 1.25kW from 1.55kW in TCT and 1.62kW in SP which increased the efficiency to 15.07% than TCT (13.84%) and SP (13.56%). From the analysis, it has been observed that the DIAR approach has enhanced the PV array power output to 11.18% more than TCT (2.11%) than the SP.

5) PARTIAL SHADING PATTERN A5
The partial shading pattern, irradiance level and shade dispersion by the DIAR approach along with power-voltage characteristics graphs have been depicted in FIGURE 7 (a). The mathematical power outputs of the TCT and DIAR have been estimated and found to be equal to $6.6I_M V_M$ however, the power output varies to a great extent. Out of the total available power of 3.26kW, the SP, TCT, and DIAR have generated 2.44kW, 2.5kW, and 2.89kW with conversion efficiencies of 74.85%, 76.69%, and 88.65% respectively. The DIAR approach encountered 2.04kW and 0.37kW of power and mismatch losses which is lower than the TCT
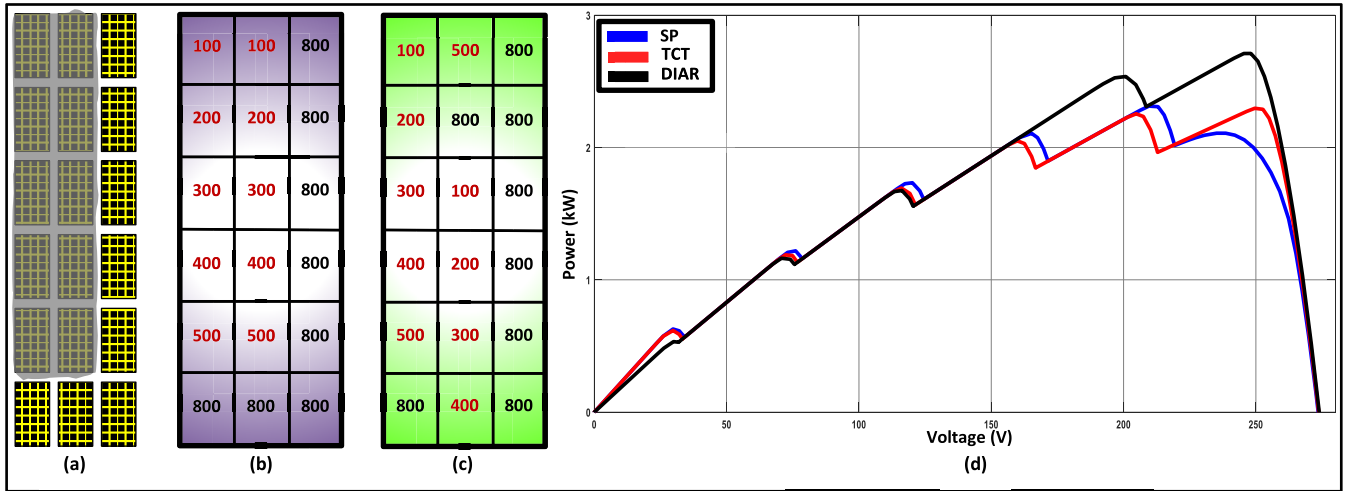
FIGURE 4. Partial shading pattern A2 for 6 × 3 PV array. (a) shading pattern, (b) irradiance in TCT and SP connection, (c) irradiance after shade dispersion by DIAR approach, and (d) power-voltage characteristics graph.

FIGURE 5. Partial shading pattern A3 for 6 × 3 PV array. (a) shading pattern, (b) irradiance in TCT and SP connection, (c) irradiance after shade dispersion by DIAR approach, and (d) power-voltage characteristics graph.
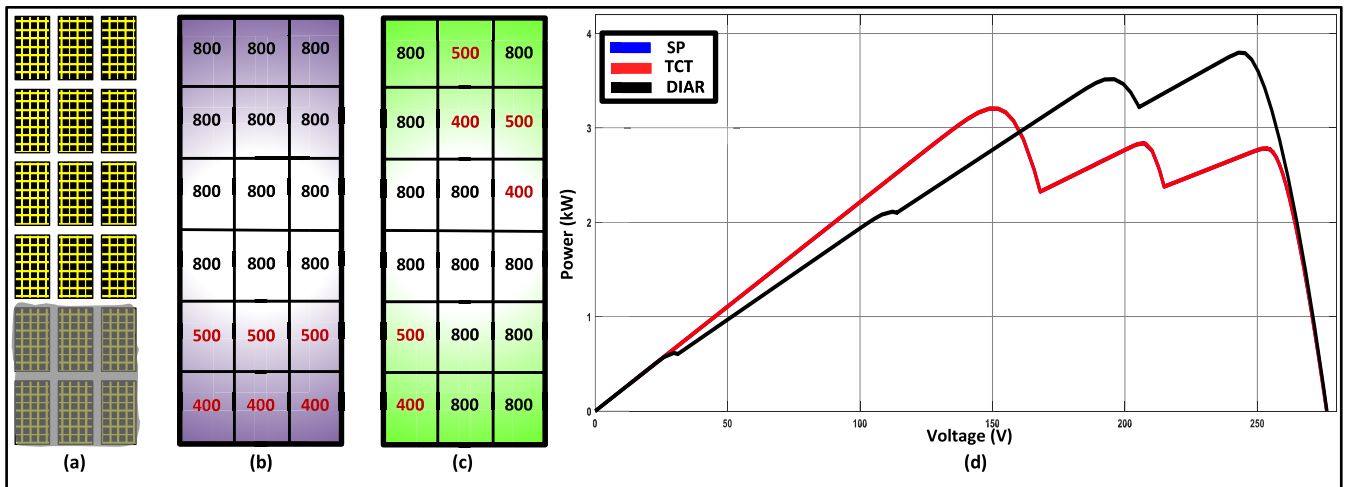
(2.43kW and 0.76kW) and SP (2.49kW and 0.82kW). The power enhancement by the TCT has been found as 2.46% whereas, for the DIAR approach, the value lies at 18.44%.

6) PARTIAL SHADING PATTERN A6

During this pattern of partial shading, the array receives lower irradiance values of 600W/m^2, 500W/m^2, 400W/m^2, and 300W/m^2 having total available power of 3.37kW. The detailed representation of the pattern, irradiance level, shade dispersion by DIAR, and the power-voltage characteristics graphs of the SP, TCT, and DIAR have been given in FIGURE 7 (b). The mathematical power estimations of the TCT and DIAR approach have been calculated as $7.2I_M V_M$ and $9I_M V_M$ respectively. The power output of the DIAR has been found to have a significantly higher value of 3.34kW than the TCT with 2.75kW and SP with 2.81kW as power output. The DIAR, TCT, and SP have power losses of 1.59kW, 2.18kW, and 2.19kW along with mismatch losses of 0.03kW, 0.62kW, and 0.56kW respectively. The DIAR

has a higher conversion efficiency of 99.11% with 18.86% higher power generation than SP whereas the TCT has a lower conversion efficiency of 81.60% with -2.14% power output than SP.

7) PARTIAL SHADING PATTERN A7

FIGURE 7 (c) represents the pictorial representation of the partial shading pattern, irradiance in SP and TCT, dispersion of partial shading by the DIAR approach, and the respective power-voltage characteristics graphs for shading pattern A7. The TCT and DIAR have the mathematical power output of $7.2I_M V_M$ and $7.8I_M V_M$ respectively. The power outputs of DIAR, TCT, and SP have been found as 3.12kW, 2.73kW, and 3.25kW from the available power of 3.37kW with conversion efficiencies as 92.58%, 81.08%, and 96.44% respectively. The DIAR has lower power (1.68kW) and mismatch (0.12kW) losses than SP (1.81kW and 0.25kW) and TCT (2.2kW and 0.64kW). The power enhancements by DIAR and TCT than the SP have been calculated
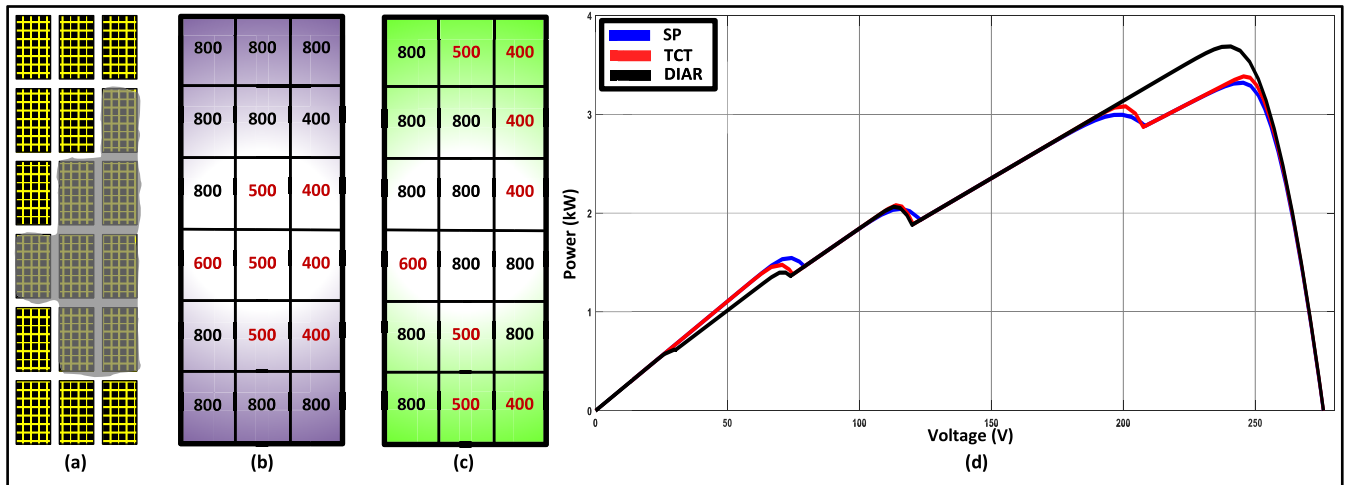
FIGURE 6. Partial shading pattern A4 for 6 × 3 PV array. (a) shading pattern, (b) irradiance in TCT and SP connection, (c) irradiance after shade dispersion by DIAR approach, and (d) power-voltage characteristics graph.

as 4.17% and -12.50% (due to lower power than SP) respectively.

8) PARTIAL SHADING PATTERN A8

The pattern, irradiance level by SP and TCT, dispersion of irradiance by DIAR approach, and the respective power-voltage characteristics graphs for the PV array under partial shading pattern A8 have been FIGURE 7 (d). The irradiances received by the modules under partial shading have been kept at values of 350W/m², 400W/m², and 480W/m². The total power in the PV array has been calculated as 2.98kW whereas the mathematical power estimation of TCT and DIAR has been found as $6.3I_MV_M$ and $6.6I_MV_M$ respectively. The DIAR approach has 2.65kW of power output with 2.28kW, 0.33kW, 88.93%, and 10.85% as power loss, mismatch loss, conversion efficiency, and efficiency than TCT (2.31kW, 2.62kW, 0.67kW, 77.52% and 9.46%) and SP (2.22kW, 2.71kW, 0.76kW, 74.50% and 9.09%) respectively.

Also, it has been found that the TCT and DIAR approach have 4.05% and 19.37% higher power generation than the SP.

The detailed summarized results obtained from the partial shading analysis of the 6 × 3 PV array with SP, TCT, and DIAR approach have been tabularized in TABLE 1. Hence, it can be concluded from this analysis that the DIAR approach has higher performance than the SP and TCT with higher power output during all the partial shading patterns.

B. 5 × 7 ASYMMETRICAL PV ARRAYS

The DIAR approach has been further applied to another asymmetrical array of 5 × 7 size and compared with total-cross-tied (TCT), honeycomb (HC), bridge-linked (BL), and series-parallel (SP) under eight different partial shading patterns. The eight patterns differ from each other in size and area along with multiple lower irradiance values ranging from 100W/m² to 600W/m² as shown in FIGURE 8. The 'U' in FIGURE 8 represents unit of 100W/m² i.e., 1U, 2U, 2.5U

and 3U denotes irradiance values of 100W/m², 200W/m², 250W/m² and 300W/m² respectively.

For partial shading pattern B1 (FIGURE 8 (a)), the theoretical power outputs from TCT and DIAR have been mathematically calculated as $21.15I_MV_M$ and $23.40I_MV_M$ respectively. The power-voltage graphs of TCT, HC, BL, SP, and DIAR have been shown in FIGURE 9 (a) in which it can be seen that out of total available power of 7.98kW, the TCT, HC BL, SP, and DIAR have power outputs as 7.46kW, 7.17kW, 7.19kW, 7.07kW, and 7.93kW respectively. The power loss, mismatch loss, conversion efficiency, power enhancement, and efficiency are found as 1.62kW, 0.52kW, 93.48%, 5.52%, and 15.71% (for TCT), 1.91kW, 0.81kW, 89.84%, 1.41% and 15.40% (for HC), 1.89kW, 0.79kW, 90.10%, 1.70% and 15.14% (for BL), 2.01kW, 0.91kW, 88.60%, 0% and 14.89% (for SP), and 1.15kW, 0.05kW, 99.37%, 12.16% and 16.70% (for DIAR) respectively.

For partial shading pattern B2 (FIGURE 8 (b)), the 5 × 7 array with the DIAR approach has a higher power output of 6.28kW than TCT (4.34kW), HC (4.26kW), BL (4.19kW), and SP (4.19kW) respectively from the total available power of 6.32kW. The power-voltage characteristics graphs of the TCT, HC, BL, SP and DIAR approach have been depicted in FIGURE 9 (b). The power and mismatch losses of the DIAR approach have been found to have lower values i.e., 2.8kW and 0.04kW than TCT (4.74kW and 1.98kW), HC (4.82kW and 2.06kW), BL and SP (4.89kW and 2.13kW) respectively. Also, the conversion efficiency and efficiency in DIAR have been noted to be higher with values equal to 99.37% and 13.22% than SP, BL (88.60% and 6.52%), HC (64.40% and 8.97%), and TCT (93.48% and 6.87%) respectively. The DIAR approach has 49.88% higher power output than SP and BL as compared to the HC (1.67%), and TCT (3.58%).

For partial shading pattern B3 (FIGURE 8 (c)), the power output of the DIAR has been noted as 6.25kW which is significantly higher than TCT (5.1kW), HC (4.97kW), BL (4.88kW) and SP (4.87kW) respectively.
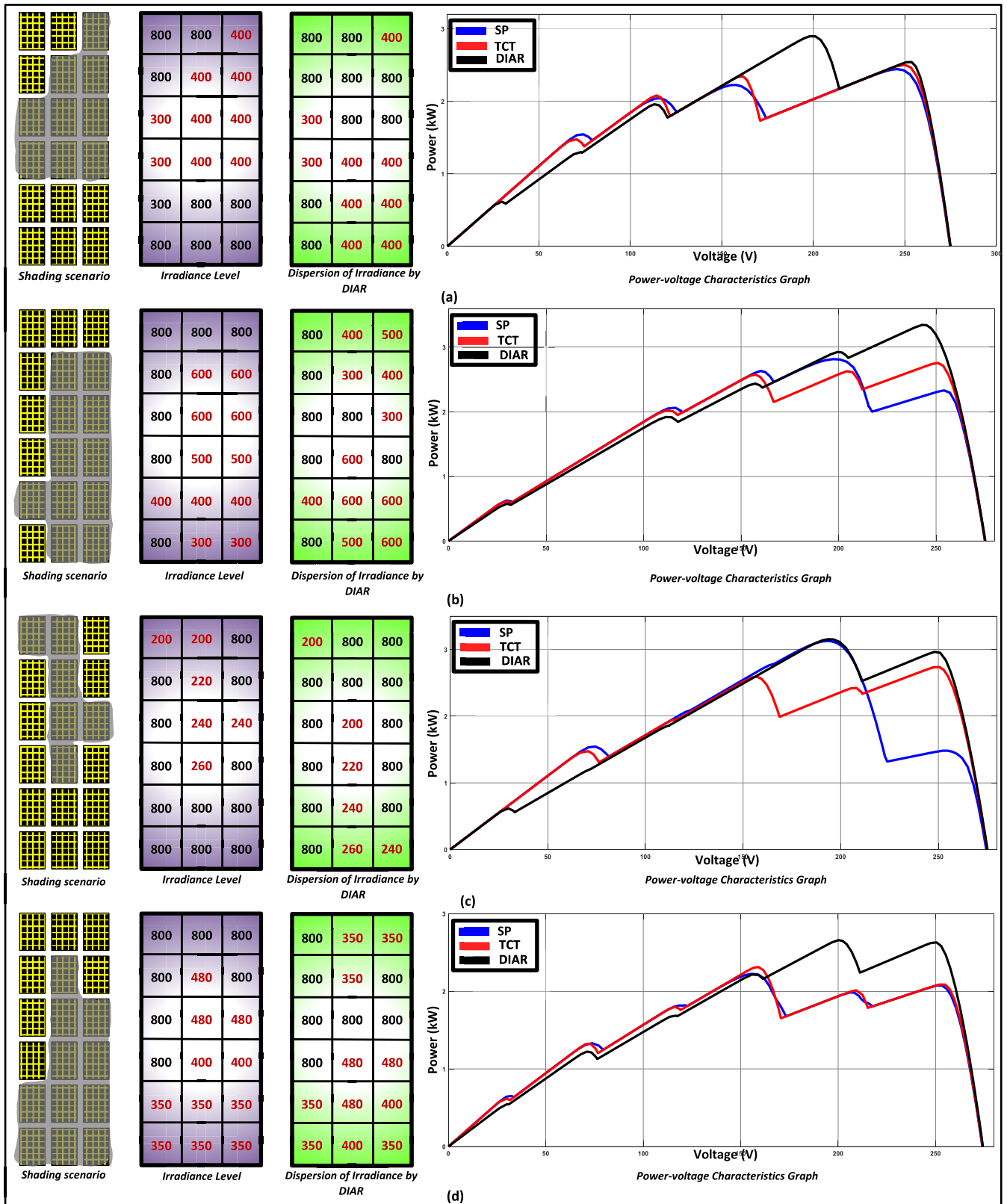
FIGURE 7. Partial shading analysis of 6 × 3 array with SP, TCT, and DIAR approach for (a) Pattern A5, (b) Pattern A6, (c) Pattern A7, and (d) Pattern A8.

The power-voltage graphs of the DIAR, TCT, HC, BL, and SP have been represented in FIGURE 9 (c) and the total

available power in the array has been calculated as 6.33kW. The TCT, HC, BL, and SP have higher power and mismatch

TABLE 1. Summarized results analysis of asymmetrical 6 × 3 PV array under partial shading patterns A1 to A8.

Partial Shading Pattern A1

PV Array	Performance Indicators								
	P_T (kW)	TP	P_O (kW)	PL (kW)	ML (kW)	LR (kW)	CE (%)	PE (%)	Eff (%)
Series-Parallel	3.71	-	3.25	1.68	0.46	0.00	87.60	0.00	13.31
Total Cross Tied		$6.6 I_M V_M$	3.2	1.73	0.51	-2.97	86.25	-1.54	13.11
DIAR		$10.2 I_M V_M$	3.69	1.24	0.02	26.19	99.46	13.54	15.11

Partial Shading Pattern A2

PV Array	Performance Indicators								
	P_T (kW)	TP	P_O (kW)	PL (kW)	ML (kW)	LR (kW)	CE (%)	PE (%)	Eff (%)
Series-Parallel	2.89	-	2.31	2.62	0.58	0.00	79.93	0.00	9.46
Total Cross Tied		$6.0 I_M V_M$	2.29	2.64	0.6	-0.76	79.24	-0.87	9.38
DIAR		$7.2 I_M V_M$	2.71	2.22	0.18	15.26	93.77	17.32	11.10

Partial Shading Pattern A3

PV Array	Performance Indicators								
	P_T (kW)	TP	P_O (kW)	PL (kW)	ML (kW)	LR (kW)	CE (%)	PE (%)	Eff (%)
Series-Parallel	3.80	-	3.2	1.73	0.6	0.00	84.21	0.00	13.11
Total Cross Tied		$7.2 I_M V_M$	3.2	1.73	0.6	0.00	84.21	0.00	13.11
DIAR		$10.2 I_M V_M$	3.79	1.14	0.01	34.10	99.74	18.44	15.52

Partial Shading Pattern A4

PV Array	Performance Indicators								
	P_T (kW)	TP	P_O (kW)	PL (kW)	ML (kW)	LR (kW)	CE (%)	PE (%)	Eff (%)
Series-Parallel	3.75	-	3.31	1.62	0.44	0.00	88.27	0.00	13.56
Total Cross Tied		$9 I_M V_M$	3.38	1.55	0.37	4.32	90.13	2.11	13.84
DIAR		$10.2 I_M V_M$	3.68	1.25	0.07	22.83	98.13	11.18	15.07

Partial Shading Pattern A5

PV Array	Performance Indicators								
	P_T (kW)	TP	P_O (kW)	PL (kW)	ML (kW)	LR (kW)	CE (%)	PE (%)	Eff (%)
Series-Parallel	3.26	-	2.44	2.49	0.82	0.00	74.85	0.00	9.99
Total Cross Tied		$6.6 I_M V_M$	2.5	2.43	0.76	2.40	76.69	2.46	10.24
DIAR		$6.6 I_M V_M$	2.89	2.04	0.37	18.07	88.65	18.44	11.84

Partial Shading Pattern A6

PV Array	Performance Indicators								
	P_T (kW)	TP	P_O (kW)	PL (kW)	ML (kW)	LR (kW)	CE (%)	PE (%)	Eff (%)
Series-Parallel	3.37	-	2.81	2.12	0.56	0.00	83.38	0.00	11.51
Total Cross Tied		$7.2 I_M V_M$	2.75	2.18	0.62	-2.83	81.60	-2.14	11.26
DIAR		$6.6 I_M V_M$	3.34	1.59	0.03	25	99.11	18.86	13.68

Partial Shading Pattern A7

PV Array	Performance Indicators								
	P_T (kW)	TP	P_O (kW)	PL (kW)	ML (kW)	LR (kW)	CE (%)	PE (%)	Eff (%)
Series-Parallel	3.37	-	3.12	1.81	0.25	0.00	92.58	0.00	12.78
Total Cross Tied		$7.2 I_M V_M$	2.73	2.2	0.64	-21.54	81.01	-12.50	11.18
DIAR		$7.8 I_M V_M$	3.25	1.68	0.12	7.18	96.44	4.17	13.31

Partial Shading Pattern A8

PV Array	Performance Indicators								
	P_T (kW)	TP	P_O (kW)	PL (kW)	ML (kW)	LR (%)	CE (%)	PE (%)	Eff (%)
Series-Parallel	2.98	-	2.22	2.71	0.76	0.00	74.50	0.00	9.09
Total Cross Tied		$6.3 I_M V_M$	2.31	2.62	0.67	03.32	77.52	4.05	9.46
DIAR		$6.6 I_M V_M$	2.65	2.28	0.33	15.86	88.93	19.37	10.85

losses as 3.98kW and 1.23kW, 4.11kW and 1.36kW, 4.2kW and 1.45kW, and 4.21kW and 1.46kW than the DIAR approach (2.83kW and 0.08kW) respectively. The conversion efficiency and power enhancement in the DIAR approach have been calculated and found to be higher (98.74% and 28.34%) than the TCT (80.57% and 4.72%), HC (78.51% and 2.05%), BL (77.09% and 0.21%) and SP (76.94% and 0%) respectively.

For partial shading pattern B4 (FIGURE 8 (d)), it can be observed from the power-voltage characteristics graphs in FIGURE 9 (d) that the DIAR approach has a higher power output of 5.93kW than TCT (4.19kW), HC (4.06kW), BL (4.1kW) and SP (3.97kW). Also, the DIAR approach has lower power and mismatch losses of 3.15kW and 0.06kW than SP (5.11kW and 2.02kW), BL (4.98kW and 1.8kW), HC (5.02kW and 1.93kW), and TCT (4.89kW and 1.8kW) respectively. The DIAR approach has 49.37% higher power than the SP whereas the HC, TCT and BL have values of 2.26%, 5.54% and 3.27% respectively. The DIAR approach has converted 99% of the total available power in the array as compared to TCT (69.95%), BL (68.45%), HC (67.77%), and SP (66.28%).

For partial shading pattern B5 (FIGURE 8 (e)), the power-voltage graphs have been depicted in FIGURE 9 (e) with power outputs of DIAR approach, TCT, HC, BL, and SP noted as 6.95kW, 6.93kW, 5.78kW 5.71kW, and 5.59kW respectively. The DIAR approach has lower power loss and mismatch loss of 2.13kW and 0.04kW with higher conversion
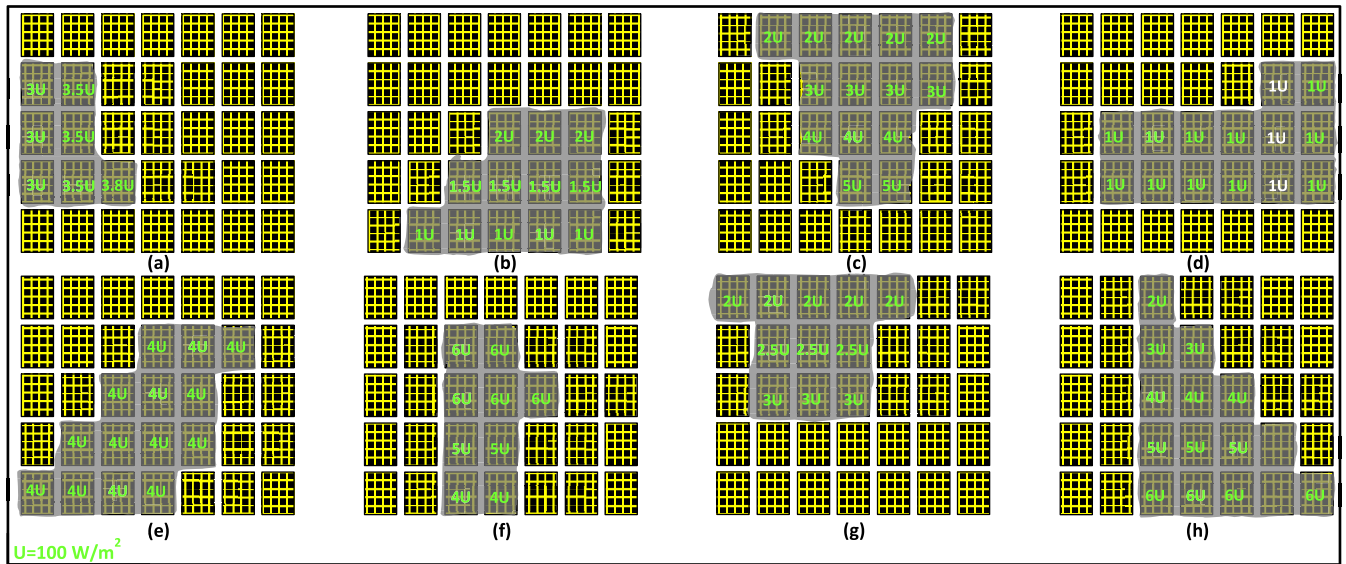
FIGURE 8. Partial shading patterns of 5 × 7 array with DIAR, TCT, BL, HC, and SP. (a) Pattern B1, (b) Pattern B2, (c) Pattern B3, (d) Pattern B4, (e) Pattern B5, (f) Pattern B6, (g) Pattern B7, and (h) Pattern B8.

efficiency and efficiency of 99.43% and 6.40% than TCT, HC, BL, and SP. Also, in terms of power enhancement capability, the DIAR approach has a higher value of 24.33% than the BL (2.15%), HC (3.39%), and TCT (23.97%).

Similarly for partial shading patterns B6 (FIGURE 8 (f)), B7 (FIGURE 8 (g)), and B8 (FIGURE 8 (h)), the power-voltage characteristics graphs have been presented in FIGURE 9 (f)-(h) respectively. From the graphs, it can be viewed that the proposed DIAR approach has significantly performed well with higher power outputs, lower power and mismatch losses with higher conversion efficiency, and power enhancement under all the partial shading patterns.

The summarized results of the 5 × 7 asymmetrical PV arrays with the DIAR approach, TCT, HC, BL, and SP for partial shading patterns have been tabularized in TABLE 2. It can be observed from the data that the DIAR approach outperformed the TCT, BL, and SP during all the partial shading patterns and hence, can be stated as the most effective in reducing the partial shading losses from the PV arrays.

C. 20 × 4 ASYMMETRICAL PV ARRAYS

The proposed DIAR approach has been further validated using a long asymmetrical PV array of 20 × 4 size (26kW system) and compared with the TCT, BL, and SP under three partial shading patterns. The shading patterns cover different areas of the PV arrays with lower irradiance values ranging from 100W/m² to 550W/m². The partial shading scenario and respective power-voltage graphs of DIAR, TCT, BL, and SP for patterns C1, C2, and C3 have been represented in FIGURE 10 (a)-(c) respectively. For pattern C1, the DIAR generated 18.41kW power output from 18.56kW available power with a conversion efficiency of 99.19%. The SP has 16.99kW power output with 91.54% conversion efficiency

whereas the TCT and BL have the same lower power output of 16.57kW with 89.28% conversion efficiency.

The DIAR approach has 8.36% higher power generation than SP whereas TCT and BL have -2.47% lower power generation than SP. For pattern C2, the total power available in the array has been calculated as 16.46kW from which the DIAR approach converted 16.37kW of power with a conversion efficiency of 99.45%. The TCT and BL have generated nearly equal powers i.e., 15.39kW and 15.4kW respectively followed by the SP of 14.72kW with conversion efficiencies of 3.94% (TCT) and 4% (BL). Similarly, for pattern C2, the TCT, BL, and SP have equal power outputs of 10.8kW however, the DIAR approach has 11.24kW as power output with 10.36% conversion efficiency.

Table 3 summarizes the detailed results obtained from the partial shading analysis of a 20 × 4 asymmetrical array with the DIAR approach, TCT, BL, and SP. It can be observed from the data that the DIAR approach has higher performance during all the partial shading patterns as compared to others.

D. 7 × 7 SYMMETRICAL PV ARRAYS

Later on, to prove the efficacy of the proposed DIAR approach to symmetrical arrays, a 7 × 7 PV array has been considered and investigated under four partial shading patterns as shown in FIGURE 11. The irradiance of the partially shaded modules has been kept at 100W/m² for all the patterns. The comparison of the DIAR approach has been done with the TCT, BL, SP, SDS [38], FER [39], henon map [40], and MS [31]. The power outputs of the PV arrays for partial shading patterns D1, D2, D3, and D4 have been noted as 7.26kW, 8.60kW, 8.1kW, and 8.12kW (for SP), 9.05kW, 9.32kW, 8.9kW and 9.17kW (for BL) and 9.15kW, 9.78kW, 8.89kW and 9.63kW (for TCT) respectively.
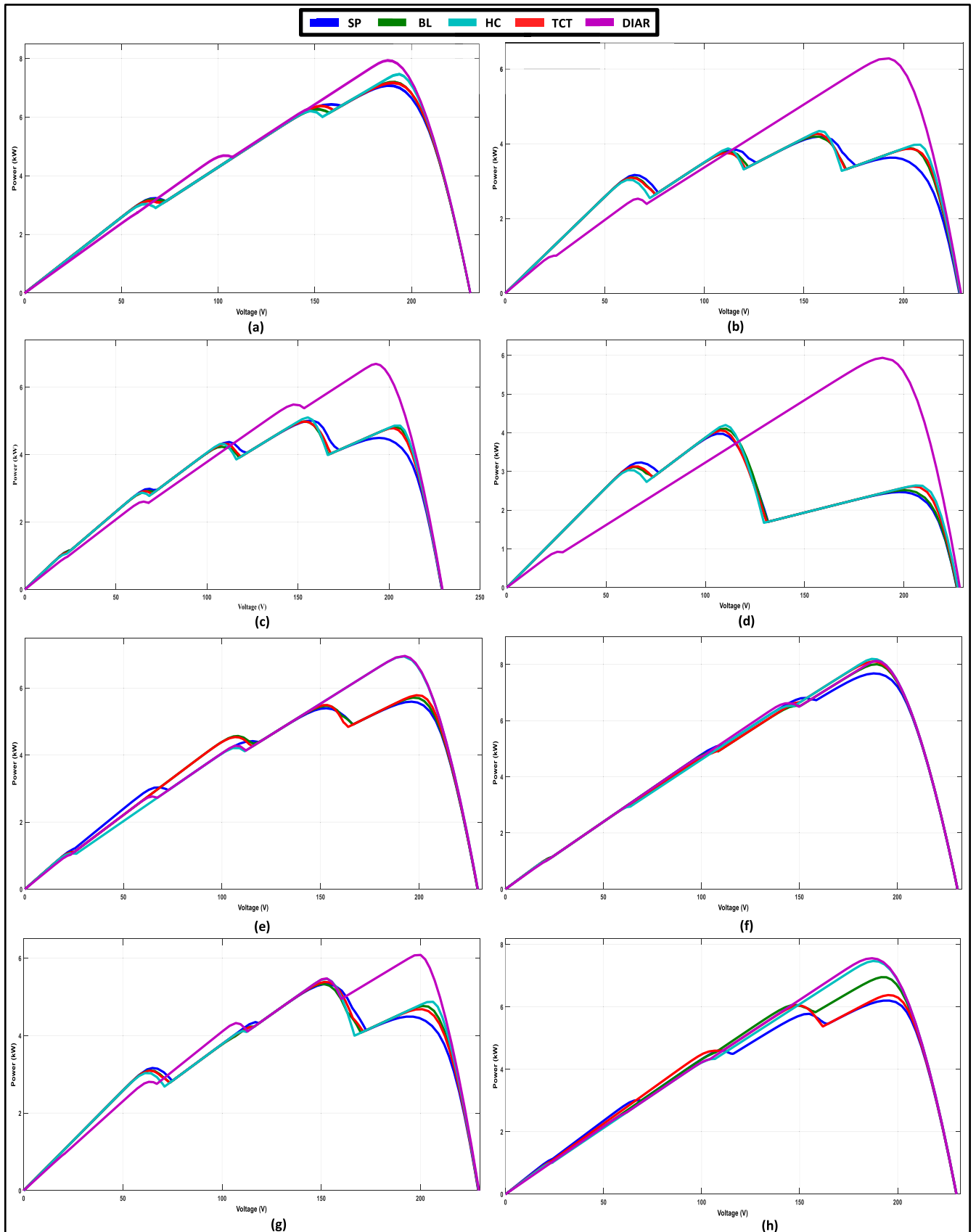
FIGURE 9. Power-voltage characteristics of 5 × 7 PV asymmetrical array with TCT, BL, HC, SP, and DIAR approach for partial shading (a) Pattern B1, (b) Pattern B2, (c) Pattern B3, (d) Pattern B4, (e) Pattern B5, (f) Pattern B6, (g) Pattern B7, and (h) Pattern B8.

TABLE 2. Summarized results analysis of asymmetrical 5 × 7 PV array under partial shading patterns B1 to B8.

Partial Shading Pattern B1

PV Array	P_T (kW)	P_O (kW)	PL (kW)	ML (kW)	LR (%)	CE (%)	PE (%)	Eff (%)
				Performance Indicators				
Series-Parallel		7.07	2.01	0.91	0.00	88.60	0.00	14.89
Bridge-Linked		7.19	1.89	0.79	5.97	90.10	1.70	15.14
Honeycomb	7.98	7.17	1.91	0.81	4.97	89.84	1.41	15.10
Total Cross Tied		7.46	1.62	0.52	19.40	93.48	5.52	15.71
DIAR		7.93	1.15	0.05	42.79	99.37	12.16	16.70

Partial Shading Pattern B2

PV Array	P_T (kW)	P_O (kW)	PL (kW)	ML (kW)	LR (%)	CE (%)	PE (%)	Eff (%)
Series-Parallel		4.19	4.89	2.13	0.00	66.30	0.00	8.82
Bridge-Linked		4.19	4.89	2.13	0.00	66.30	0.00	8.82
Honeycomb	6.32	4.26	4.82	2.06	1.43	67.40	1.67	8.97
Total Cross Tied		4.34	4.74	1.98	3.07	68.67	3.58	9.14
DIAR		6.28	2.8	0.04	42.74	99.37	49.88	13.22

Partial Shading Pattern B3

PV Array	P_T (kW)	P_O (kW)	PL (kW)	ML (kW)	LR (kW)	CE (%)	PE (%)	Eff (%)
Series-Parallel		4.87	4.21	1.46	0.00	76.94	0.00	10.25
Bridge-Linked		4.88	4.2	1.45	0.24	77.09	0.21	10.27
Honeycomb	6.33	4.97	4.11	1.36	2.38	78.51	2.05	10.46
Total Cross Tied		5.1	3.98	1.23	5.46	80.57	4.72	10.74
DIAR		6.25	2.83	0.08	32.78	98.74	28.34	13.16

Partial Shading Pattern B4

PV Array	P_T (kW)	P_O (kW)	PL (kW)	ML (kW)	LR (kW)	CE (%)	PE (%)	Eff (%)
Series-Parallel		3.97	5.11	2.02	0.00	66.28	0.00	8.36
Bridge-Linked		4.1	4.98	1.89	2.54	68.45	3.27	8.63
Honeycomb	5.99	4.06	5.02	1.93	1.76	67.77	2.26	8.55
Total Cross Tied		4.19	4.89	1.8	4.31	69.95	5.54	8.82
DIAR		5.93	3.15	0.06	38.36	99.00	49.37	12.49

Partial Shading Pattern B5

PV Array	P_T (kW)	P_O (kW)	PL (kW)	ML (kW)	LR (kW)	CE (%)	PE (%)	Eff (%)
Series-Parallel		5.59	3.49	1.4	0.00	79.97	0.00	11.77
Bridge-Linked		5.71	3.37	1.28	3.44	81.69	2.15	12.02
Honeycomb	6.99	5.78	3.30	1.21	5.44	82.68	3.39	12.17
Total Cross Tied		6.93	2.15	0.06	38.40	99.14	23.97	14.59
DIAR		6.95	2.13	0.04	38.97	99.43	24.33	14.63

Partial Shading Pattern B6

PV Array	P_T (kW)	P_O (kW)	PL (kW)	ML (kW)	LR (kW)	CE (%)	PE (%)	Eff (%)
Series-Parallel		7.67	1.41	0.65	0.00	92.19	0.00	16.15
Bridge-Linked		7.89	1.19	0.43	15.60	94.83	2.87	16.61
Honeycomb	8.07	7.91	1.17	0.16	22.70	98.01	3.12	16.66
Total Cross Tied		7.99	1.09	0.33	41.84	96.03	4.17	16.82
DIAR		8.26	0.82	0.06		99.28	7.69	17.39

Partial Shading Pattern B7

PV Array	P_T (kW)	P_O (kW)	PL (kW)	ML (kW)	LR (kW)	CE (%)	PE (%)	Eff (%)
Series-Parallel		5.33	3.75	1.19	0.00	81.75	0.00	11.22
Bridge-Linked		5.33	3.75	1.19	0.00	81.75	0.00	11.22
Honeycomb	6.52	5.38	3.70	1.14	1.33	82.51	0.93	11.33
Total Cross Tied		5.46	3.62	1.06	3.47	83.74	2.44	11.50
DIAR		6.08	3	0.44	20.00	93.25	14.07	12.80

Partial Shading Pattern B8

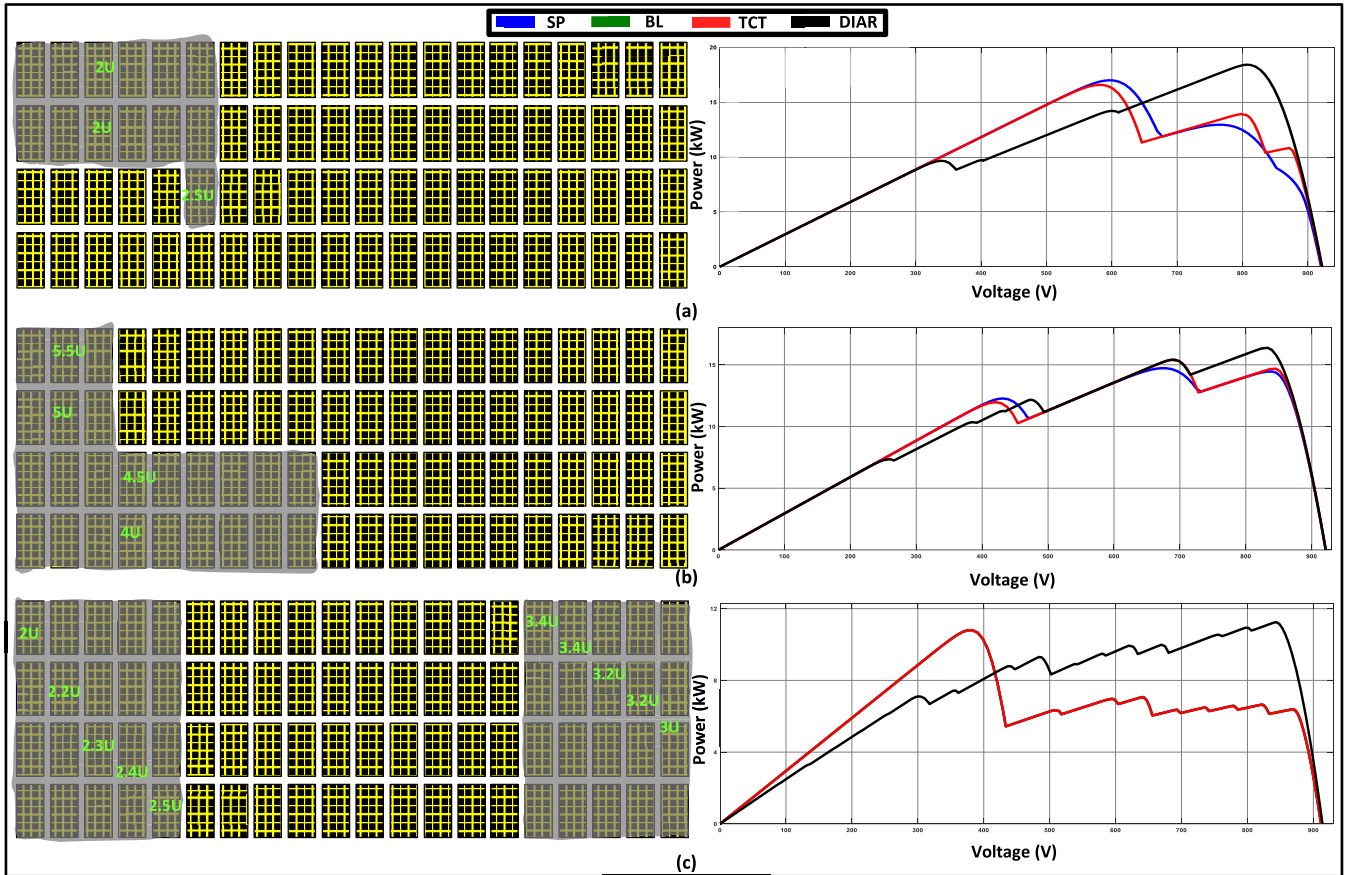| PV Array	P_T (kW)	P_O (kW)	PL (kW)	ML (kW)	LR (%)	CE (%)	PE (%)	Eff (%)
Series-Parallel		6.44	2.64	1.21	0.00	84.18	0.00	13.56
Bridge-Linked		7.08	2	0.57	24.24	92.55	9.94	14.91
Honeycomb	7.65	6.37	2.71	1.28	-2.67	83.26	16.30	13.41
Total Cross Tied		7.49	1.59	0.16	39.77	97.91	17.70	15.77
DIAR		7.58	1.5	0.07	43.18	99.08		15.79

FIGURE 10. Partial shading patterns and power-voltage characteristics graphs of 20 × 4 asymmetrical PV arrays with DIAR, TCT, BL, and SP. (a) Pattern C1, (b) Pattern C2, and (c) Pattern C3.

TABLE 3. Summarized results analysis of asymmetrical 20 × 4 PV array under partial shading patterns C1 to C3.

PV Array	Partial Shading Pattern C1							
	Performance Indicators							
	P_T (kW)	P_O (kW)	PL (kW)	ML (kW)	LR (%)	CE (%)	PE (%)	Eff (%)
Series-Parallel	18.56	16.99	5.35	1.57	0.00	91.54	0.00	15.66
Bridge-Linked		16.57	5.77	1.99	-7.85	89.28	-2.47	15.27
Total Cross Tied		16.57	5.77	1.99	-7.85	89.28	-2.47	15.27
DIAR		18.41	3.93	0.15	26.54	99.19	8.36	16.96

PV Array	Partial Shading Pattern C2							
	Performance Indicators							
	P_T (kW)	P_O (kW)	PL (kW)	ML (kW)	LR (%)	CE (%)	PE (%)	Eff (%)
Series-Parallel	16.46	14.72	7.62	1.74	0.00	89.43	0.00	13.56
Bridge-Linked		15.4	6.94	1.06	8.92	93.56	4.00	14.19
Total Cross Tied		15.39	6.95	1.07	8.79	93.50	3.94	14.18
DIAR		16.37	5.97	0.09	21.65	99.45	9.71	15.08

PV Array	Partial Shading Pattern C3							
	Performance Indicators							
	P_T (kW)	P_O (kW)	PL (kW)	ML (kW)	LR (kW)	CE (%)	PE (%)	Eff (%)
Series-Parallel	11.36	10.8	11.54	0.56	0.00	95.07	0.00	9.95
Bridge-Linked		10.8	11.54	0.56	0.00	95.07	0.00	9.95
Total Cross Tied		10.8	11.54	0.56	0.00	95.07	0.00	9.95
DIAR		11.24	11.1	0.12	3.81	98.94	4.07	10.36

It has been noted that the PV array with SDS, FER, henon map, and MS have generated nearly equal power outputs of 10.67kW, 9.92kW, 9.41kW, and 9.85kW for partial shading patterns D1, D2, D3, and D4 respectively. In the case of the DIAR approach, the power generation for partial shading

patterns D2 and D3 are the same as that of SDS, FER, henon map, and MS i.e., 9.92kW and 9.41kW respectively. But, the DIAR has slightly higher power output than the above-mentioned reconfiguration techniques during partial shading patterns D1 and D4 with power output values of
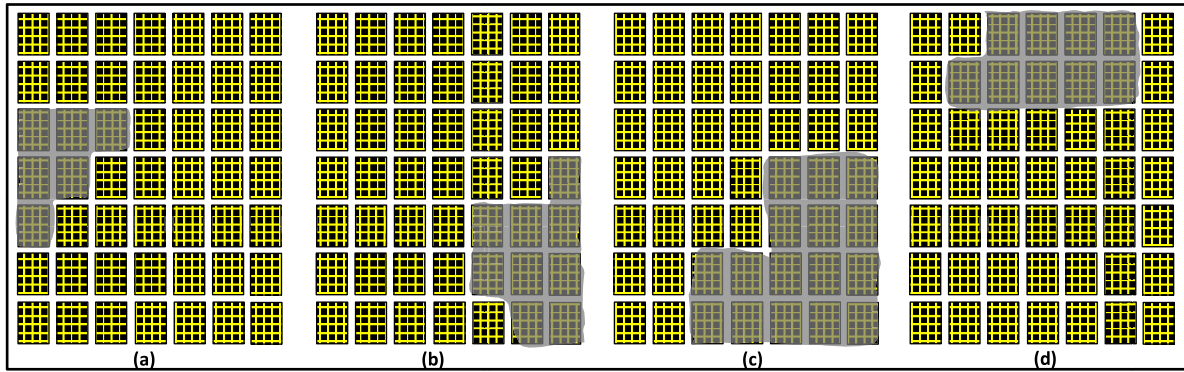
FIGURE 11. Partial shading patterns (a) D1, (b) D2, (c) D3, and (d) D4 for 7 × 7 symmetrical PV array.
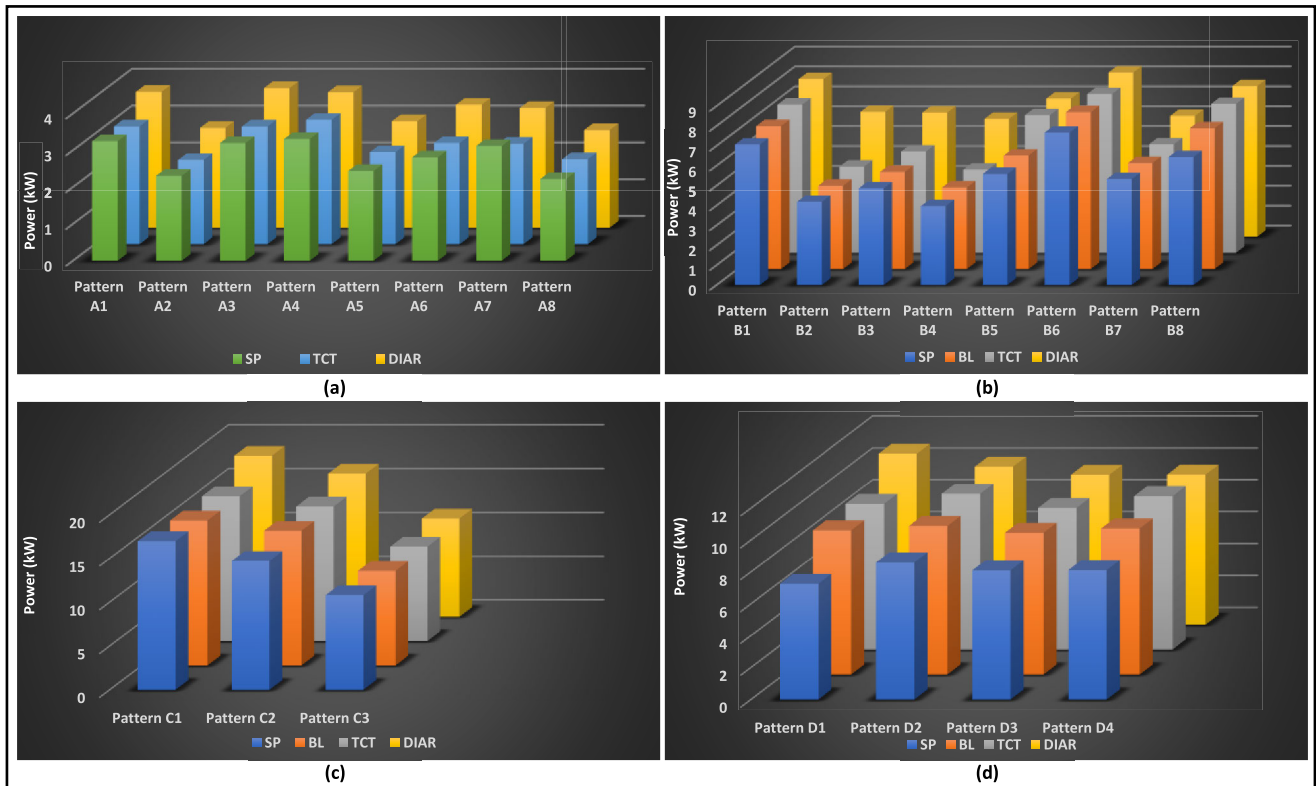

FIGURE 12. Power output comparison of DIAR approach, TCT, BL, and SP under different partial shading patterns for (a) 6 × 3, (b) 5 × 7, (c) 20 × 4, and (d) 7 × 7 PV arrays.

10.73kW and 9.92kW respectively. Hence, from the analysis, it can be stated that the DIAR can effectively work for symmetrical PV arrays and can either generate higher power or equal power to that of TCT, BL, SP, and other four symmetrical reconfiguration techniques.

The graphical comparison of the power output comparison of the DIAR approach with TCT, BL, and SP during different partial shading patterns for 6 × 3, 5 × 7, 20 × 4, and 7 × 7 PV arrays have been shown in FIGURE 12 (a)-(d) respectively. It can be viewed from the graphs that the proposed DIAR approach has higher power generation during all the partial shading patterns irrespective of the array size and structure i.e., symmetric or asymmetric. Also, a graphical comparison

of the power enhancement by the DIAR approach, TCT, and BL to the SP during all the partial shading patterns for 6 × 3, 5 × 7, 20 × 4, and 7 × 7 PV arrays has been conducted in FIGURE 13 (a)-(d) respectively. From the graph, it can be observed that the DIAR has higher power enhancement during partial shading than any other array architecture. The negative power enhancement data replicate the array with lower power output than the SP.

In addition, to support the simulation analysis, an experimental investigation has been conducted for a 4 × 3 PV array under different partial shading patterns with TCT, BL, SP, and DIAR approach. The experimental setup has been given in FIGURE 14 with twelve modules
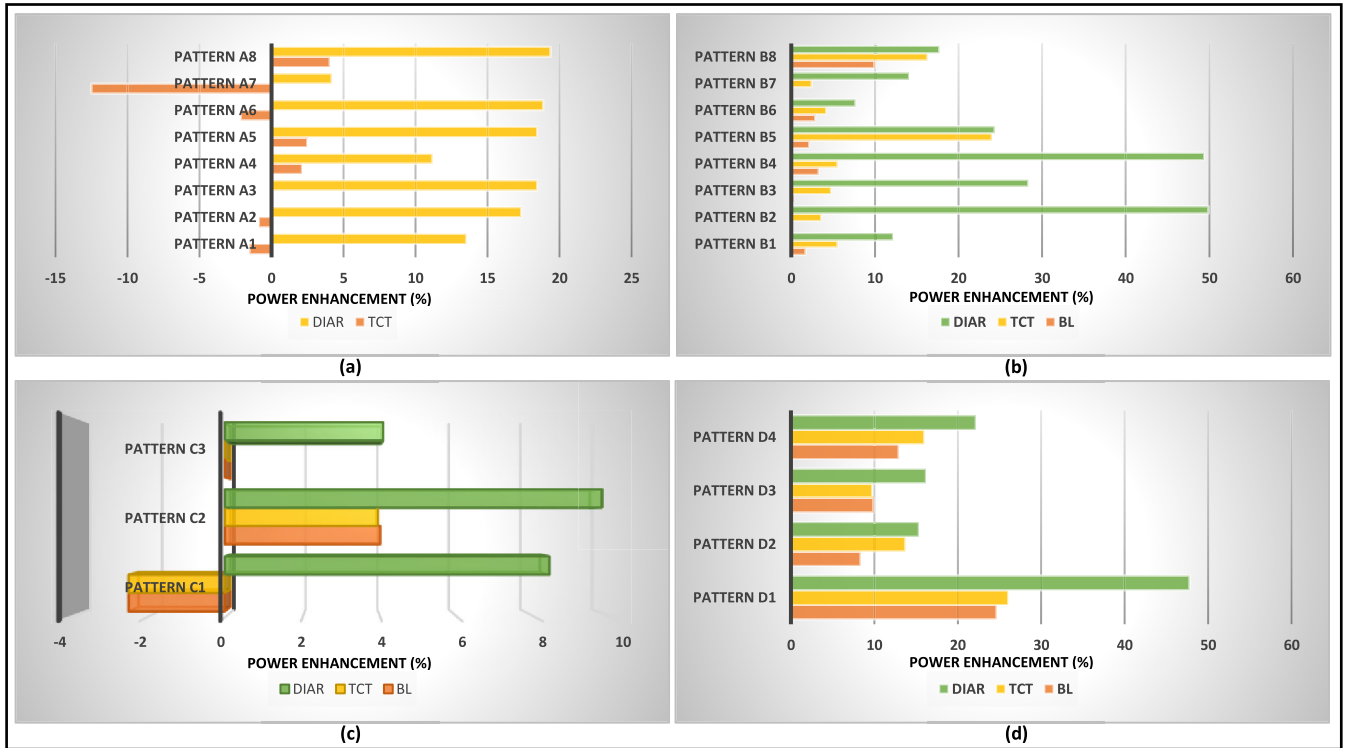
FIGURE 13. Power enhancement by DIAR approach, TCT, and BL to SP under different partial shading patterns for (a) 6 × 3, (b) 5 × 7, (c) 20 × 4, and (d) 7 × 7 PV arrays.
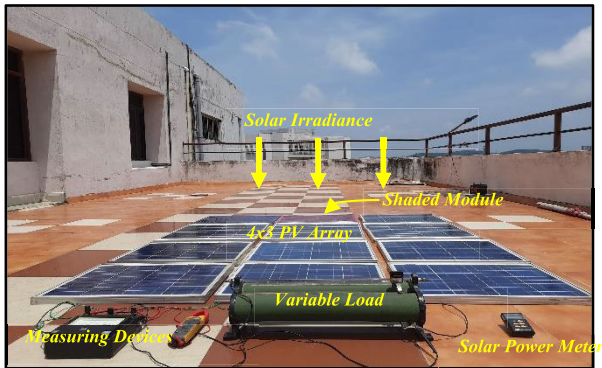

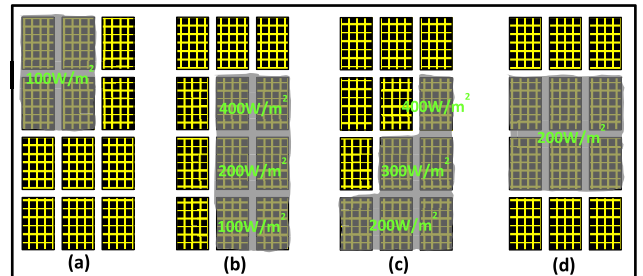**FIGURE 14.** Experimental prototype of a 4 × 3 PV array.

FIGURE 15. Partial shading patterns for experimental validation of 4 × 3 array.

each rated as 50W (maximum power), 17.5V (maximum voltage), and 2.87A (maximum current) at STC to form PV arrays.

The array has been connected to a variable resistor (rheostat) of 220Ω and 20A rating through a voltmeter (0-200V) and multimeter (Fluke 376 True RMS Clamp Meter) for voltage and current measurement. The solar irradiance received by the modules has been measured using a solar power meter (TES-1333) whereas the module temperature is recorded using an infrared thermometer (STA380A, -32°C to 380°C). The TCT, BL, and SP have been applied by changing the connection between the modules whereas the DIAR approach has been applied by permanently changing the positions of the modules.

The power-voltage graph has been extracted from the voltage and current data recorded by varying the rheostat from a lower to a higher range. The experiment has been conducted at the E-block roof, ITER, Bhubaneswar (20.2961°N, 85.8245°E) during noon hours where the maximum irradiance received by the modules at horizontal plane has been recorded as 800-820W/m² irrespective of the tilt angle of the location with an ambient temperature of 32°C. The partial shading scenarios have been created by using transparent color sheets that act as barriers between the irradiance and the modules and hence, reduce the receiving irradiance of the target module. A slight deviation between the simulation and experiments results has been noted which occurs due to various factors such as fluctuating irradiance in the site, temperature difference between the modules and modules internal mismatches that cannot be avoided while operation at field.
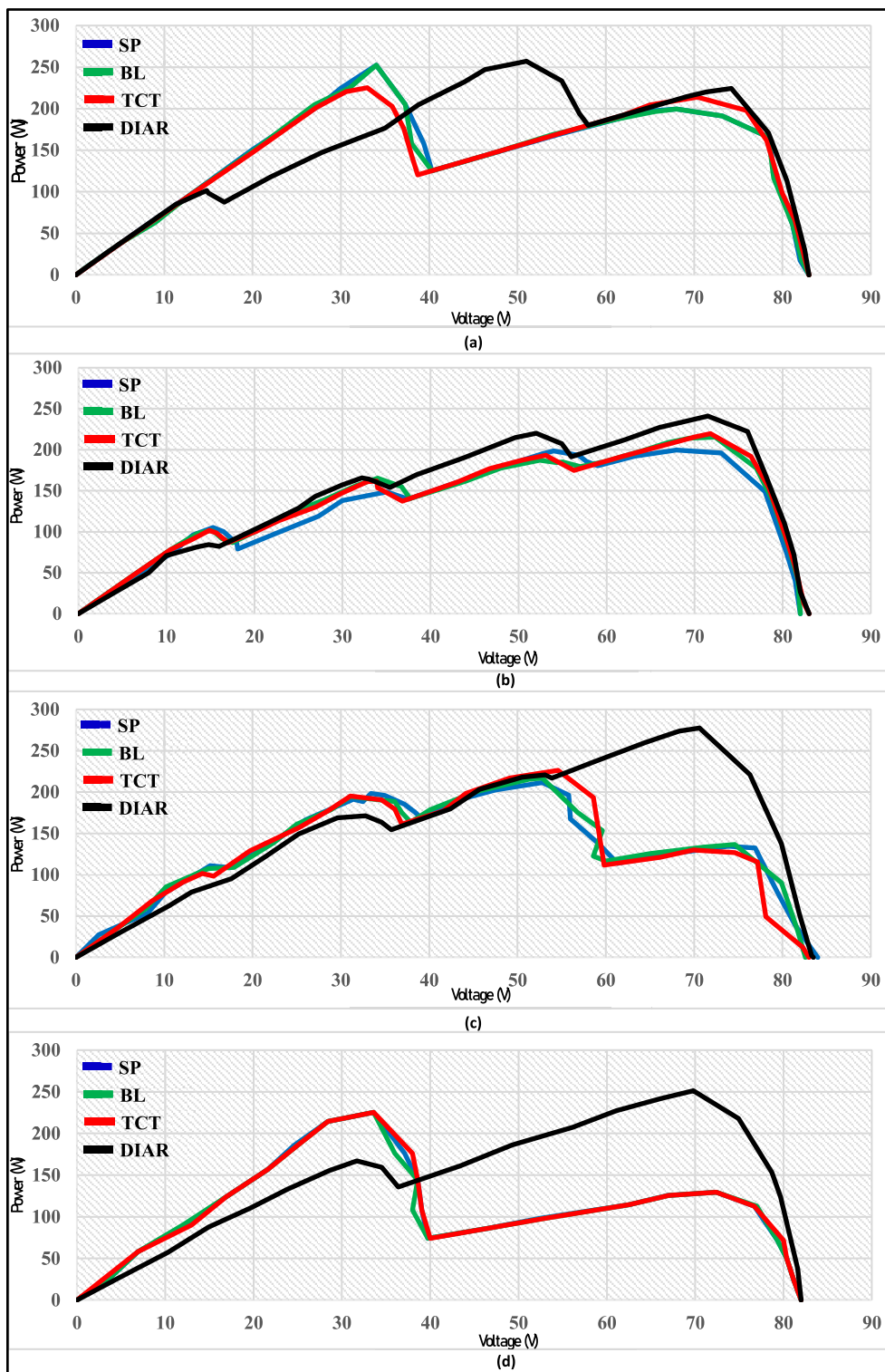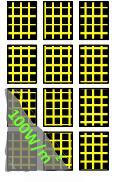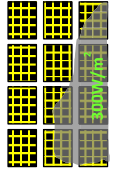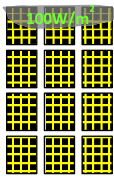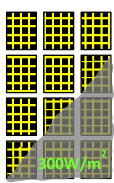
FIGURE 16. Power-voltage graphs of the 4 × 3 PV array with DIAR approach, TCT, BL, and SP plotted from the experimental data.

The partial shading patterns used for the validation of the 4 × 3 array have been shown in FIGURE 15. The power-voltage graphs obtained from the experimental analysis of the 4 × 3 PV array for partial shading patterns E1 (FIGURE 15 (a)), E2 (FIGURE 15 (b)), E3 (FIGURE 15 (c)) and E4 (FIGURE 15 (d)) have been plotted in FIGURE 16 (a), (b), (c) and (d) respectively. The power outputs of the array under partial shading pattern E1 have been noted as 232.32W (SP and BL), 225.22W (TCT), and 257.07W (DIAR approach). Similarly, for patterns

TABLE 4. Summarized results analysis of 4 × 3 under various cell-level shading scenarios.

Partial Shading Patterns	Performance Indicators	PV Arrays			
		Series-Parallel	Bridge-Linked	Total Cross Tied	DIAR
	Po(W)	261.25	251.15	265.55	336.36
	PL (W)	207.36	217.56	203.16	132.35
	ML (W)	100.3	110.50	96.10	25.29
	LR (W)	0	-10.2	4.2	75.01
	CE (%)	72.27	69.45	73.43	93.01
	PE (%)	0	-3.86	1.64	28.75
	Eff (%)	7.15	6.87	7.26	9.20
	Po(W)	217.49	225.82	232.16	237.54
	PL (W)	251.22	242.89	236.55	231.17
	ML (W)	63.87	55.54	49.20	43.82
	LR (W)	0	8.33	14.67	20.02
	CE (%)	77.30	80.26	82.51	84.43
	PE (%)	-	3.83	6.74	9.21
	Eff (%)	5.95	6.17	6.35	6.49
	Po(W)	348.94	348.94	348.94	356.54
	PL (W)	119.77	119.77	119.77	112.17
	ML (W)	10.37	10.37	10.37	2.77
	LR (W)	0	0	0	7.6
	CE (%)	97.11	97.11	97.11	99.23
	PE (%)	0	0	0	2.17
	Eff (%)	9.54	9.54	9.54	9.75
	Po(W)	209.55	193.86	210.84	225.3
	PL (W)	259.16	274.85	257.87	243.41
	ML (W)	80.19	95.88	78.90	64.44
	LR (W)	0	-14.99	48.32	15.55
	CE (%)	72.32	66.91	72.77	77.76
	PE (%)	0	-7.48	0.61	7.51
	Eff (%)	5.73	5.30	5.76	6.16

E2, E3, and E4, the DIAR approach have the higher power output recorded as 241.12W, 277.56W, and 251.20W respectively. The TCT has the power output recorded as 219.65W and 226.26W for partial shading patterns E2 and E3 respectively followed by BL (216.21W and 218.18W) and SP (200.12W and 211.59W). For pattern E4, the TCT, BL, and SP have equal power outputs recorded as 225.22W. Additionally, various cell-level shading scenarios have been considered for further performance investigation of the DIAR approach and the results are summarized in Table 4. It has been noted that the proposed approach has enhanced the power output of the array during all shading cases with a higher conversion rate as compared to the TCT, BL, and SP arrays.

Hence, from the above-conducted analysis of partial shading in 6×3, 5×7, 20×4, 7×7, and 4×3 PV arrays, it can be stated that the DIAR approach has significantly performed very well during all partial shading patterns. The approach has generated higher power than the TCT, BL, SP, and other reconfiguration strategies during partial shading and hence can be an effective solution for partial shading loss reduction in PV arrays.

V. CONCLUSION

A novel Dimension-Independent Array Relocation (DIAR) approach has been proposed in this paper that can reduce the losses in the PV array during partial shading. The effectiveness of the proposed has been studied using three asymmetrical arrays of 6 × 3, 5 × 7, 20 × 4, and 4 × 3 (experimental analysis) sizes along with a 7 × 7 symmetrical array under numerous partial shading patterns. The performance comparison of the DIAR approach has been done with the TCT, BL, HC, SP, and various reconfiguration strategies using various parameters and power-voltage graphs. From the conducted investigation, the following novelty and conclusions have been drawn:

➢ DIAR approach has higher power output for all the partial shading patterns.
➢ DIAR approach minimizes the power and mismatch losses in the array during partial shading patterns.
➢ DIAR has an average conversation efficiency of 96% for 6 × 3 array, 98.44% for 5 × 7 array, 99.19% for 20 × 4 array, and 98.54% for 7 × 7 array which is notably higher than other architectures.
➢ DIAR has higher power output (enhancement) of 15.16%, 25.44%, 7.38%, and 25.36% on average for 6 × 3, 5 × 7, 20 × 4, and 7 × 7 PV arrays than other architectures.
➢ DIAR approach has been experimentally tested for 4 × 3 PV array and found to have effective in higher power generation during partial shading than TCT, BL, and SP.
➢ TCT is incapable of generating higher power during every partial shading pattern.

➢ DIAR increases the efficiency of the PV array during partial shading.

➢ DIAR approach is applicable for both symmetrical and asymmetrical arrays and can enhance power generation during partial shading.

➢ DIAR generated higher power output than existing TCT, HC, BL, SP, SDS, FER, Henon Map and MS techniques.

➢ DIAR utilizes no sensors, switches, or complex algorithms for implementation.

➢ DIAR is a user-friendly, less complex, and low-cost solution for partial shading losses reduction in PV arrays.

REFERENCES

[1] A. Aslam, N. Ahmed, S. A. Qureshi, M. Assadi, and N. Ahmed, "Advances in solar PV systems; A comprehensive review of PV performance, influencing factors, and mitigation techniques," *Energies*, vol. 15, no. 20, p. 7595, 2022.

[2] L. Polleux, G. Guerassimoff, J.-P. Marmorat, J. Sandoval-Moreno, and T. Schuhler, "An overview of the challenges of solar power integration in isolated industrial microgrids with reliability constraints," *Renew. Sustain. Energy Rev.*, vol. 155, Mar. 2022, Art. no. 111955.

[3] M. Elahi, H. M. Ashraf, and C.-H. Kim, "An improved partial shading detection strategy based on chimp optimization algorithm to find global maximum power point of solar array system," *Energies*, vol. 15, no. 4, p. 1549, Feb. 2022.

[4] V. Balaji and A. P. Fathima, "Hybrid algorithm for MPPT tracking using a single current sensor for partially shaded PV systems," *Sustain. Energy Technol. Assessments*, vol. 53, Oct. 2022, Art. no. 102415.

[5] M. U. Ali, S. Saleem, H. Masood, K. D. Kallu, M. Masud, M. J. Alvi, and A. Zafar, "Early hotspot detection in photovoltaic modules using color image descriptors: An infrared thermography study," *Int. J. Energy Res.*, vol. 46, no. 2, pp. 774–785, Feb. 2022.

[6] A. Mäki and S. Valkealahti, "Power losses in long string and parallel-connected short strings of series-connected silicon-based photovoltaic modules due to partial shading conditions," *IEEE Trans. Energy Convers.*, vol. 27, no. 1, pp. 173–183, Mar. 2012.

[7] O. Bingöl and B. Özkaya, "Analysis and comparison of different PV array configurations under partial shading conditions," *Sol. Energy*, vol. 160, pp. 336–343, Jan. 2018.

[8] P. R. Satpathy, A. Sarangi, S. Jena, B. Jena, and R. Sharma, "Topology alteration for output power maximization in PV arrays under partial shading," in *Proc. Technol. Smart-City Energy Secur. Power (ICSESP)*, Mar. 2018, pp. 1–6.

[9] P. R. Satpathy, P. Bhowmik, T. S. Babu, R. Sharma, and C. Sain, "Bypass diodes configurations for mismatch losses mitigation in solar PV modules," in *Innovation in Electrical Power Engineering, Communication, and Computing Technology*. Singapore: Springer, 2022, pp. 197–208.

[10] P. R. Satpathy, S. Jena, and R. Sharma, "Power enhancement from partially shaded modules of solar PV arrays through various interconnections among modules," *Energy*, vol. 144, pp. 839–850, Feb. 2018.

[11] M. Matam and V. R. Barry, "Improved performance of dynamic photovoltaic array under repeating shade conditions," *Energy Convers. Manag.*, vol. 168, pp. 639–650, Jul. 2018.

[12] M. Karakose, M. Baygin, K. Murat, N. Baygin, and E. Akin, "Fuzzy based reconfiguration method using intelligent partial shadow detection in PV arrays," *Int. J. Comput. Intell. Syst.*, vol. 9, no. 2, pp. 202–212, 2016.

[13] A. Chaouachi, R. M. Kamel, and K. Nagasaka, "Microgrid efficiency enhancement based on neuro-fuzzy MPPT control for photovoltaic generator," in *Proc. 35th IEEE Photovoltaic Specialists Conf.*, Jun. 2010, pp. 002889–002894.

[14] P. Dos Santos, E. M. Vicente, and E. R. Ribeiro, "Reconfiguration methodology of shaded photovoltaic panels to maximize the produced energy," in *Proc. 11th Brazilian Power Electron. Conf.*, Sep. 2011, pp. 700–706.

[15] E. R. Sanseverino, T. N. Ngoc, M. Cardinale, V. Li Vigni, D. Musso, P. Romano, and F. Viola, "Dynamic programming and Munkres algorithm for optimal photovoltaic arrays reconfiguration," *Sol. Energy*, vol. 122, pp. 347–358, Dec. 2015.

[16] K. S. Parlak, "PV array reconfiguration method under partial shading conditions," *Int. J. Electr. Power Energy Syst.*, vol. 63, pp. 713–721, Dec. 2014.

[17] Y. Mahmoud and E. El-Saadany, "Fast reconfiguration algorithm for improving the efficiency of PV systems," in *Proc. 8th Int. Renew. Energy Congr. (IREC)*, Mar. 2017, pp. 1–5.

[18] S. N. Deshkar, S. B. Dhale, J. S. Mukherjee, T. S. Babu, and N. Rajasekar, "Solar PV array reconfiguration under partial shading conditions for maximum power extraction using genetic algorithm," *Renew. Sustain. Energy Rev.*, vol. 43, pp. 102–110, Mar. 2015.

[19] T. S. Babu, J. P. Ram, T. Dragicevic, M. Miyatake, F. Blaabjerg, and N. Rajasekar, "Particle swarm optimization based solar PV array reconfiguration of the maximum power extraction under partial shading conditions," *IEEE Trans. Sustain. Energy*, vol. 9, no. 1, pp. 74–85, Jan. 2018.

[20] A. Fathy, "Recent meta-heuristic grasshopper optimization algorithm for optimal reconfiguration of partially shaded PV array," *Sol. Energy*, vol. 171, pp. 638–651, Sep. 2018.

[21] B. Aljafari, P. R. Satpathy, and S. B. Thanikanti, "Partial shading mitigation in PV arrays through dragonfly algorithm based dynamic reconfiguration," *Energy*, vol. 257, Oct. 2022, Art. no. 124795.

[22] D. Yousri, D. Allam, and M. B. Eteiba, "Optimal photovoltaic array reconfiguration for alleviating the partial shading influence based on a modified Harris hawks optimizer," *Energy Convers. Manag.*, vol. 206, Feb. 2020, Art. no. 112470.

[23] S. K. Cherukuri and S. R. Rayapudi, "Enhanced grey wolf optimizer based MPPT algorithm of PV system under partial shaded condition," *Int. J. Renew. Energy Develop.*, vol. 6, no. 3, p. 203, Nov. 2017.

[24] A. Fathy, "Butterfly optimization algorithm based methodology for enhancing the shaded photovoltaic array extracted power via reconfiguration process," *Energy Convers. Manag.*, vol. 220, Sep. 2020, Art. no. 113115.

[25] P. R. Satpathy, P. Bhowmik, T. S. Babu, C. Sain, R. Sharma, and H. H. Alhelou, "Performance and reliability improvement of partially shaded PV arrays by one-time electrical reconfiguration," *IEEE Access*, vol. 10, pp. 46911–46935, 2022.

[26] D. Manimegalai, M. Karthikeyan, and S. C. Vijayakumar, "Maximizing power output of partially shaded photovoltaic arrays using SuDoKu configuration," *ARPN J. Eng. Appl. Sci.*, vol. 13, no. 1, pp. 124–133, 2018.

[27] S. G. Krishna and T. Moger, "Optimal SuDoKu reconfiguration technique for total-cross-tied PV array to increase power output under non-uniform irradiance," *IEEE Trans. Energy Convers.*, vol. 34, no. 4, pp. 1973–1984, Dec. 2019.

[28] G. Sai Krishna and T. Moger, "Improved SuDoKu reconfiguration technique for total-cross-tied PV array to enhance maximum power under partial shading conditions," *Renew. Sustain. Energy Rev.*, vol. 109, pp. 333–348, Jul. 2019.

[29] V. M. R. Tatabhatla, A. Agarwal, and T. Kanumuri, "Enhanced performance metrics under shading conditions through experimental investigations," *IET Renew. Power Gener.*, vol. 14, no. 14, pp. 2592–2603, Oct. 2020.

[30] M. S. S. Nihanth, J. P. Ram, D. S. Pillai, A. M. Y. M. Ghias, A. Garg, and N. Rajasekar, "Enhanced power production in PV arrays using a new skyscraper puzzle based one-time reconfiguration procedure under partial shade conditions (PSCs)," *Sol. Energy*, vol. 194, pp. 209–224, Dec. 2019.

[31] G. H. K. Varma, V. R. Barry, and R. K. Jain, "A novel magic square based physical reconfiguration for power enhancement in larger size photovoltaic array," *IETE J. Res.*, pp. 1–14, Jul. 2021.

[32] N. Rakesh and T. V. Madhavaram, "Performance enhancement of partially shaded solar PV array using novel shade dispersion technique," *Frontiers Energy*, vol. 10, no. 2, pp. 227–239, Jun. 2016.

[33] S. M. Samikannu, R. Namani, and S. K. Subramaniam, "Power enhancement of partially shaded PV arrays through shade dispersion using magic square configuration," *J. Renew. Sustain. Energy*, vol. 8, no. 6, Nov. 2016, Art. no. 063503.

[34] L. El Iysaouy, M. Lahbabi, and A. Oumnad, "A novel magic square view topology of a PV system under partial shading condition," *Energy Proc.*, vol. 157, pp. 1182–1190, Jan. 2019.

[35] S. S. Reddy and C. Yammani, "Odd-even-prime pattern for PV array to increase power output under partial shading conditions," *Energy*, vol. 213, Dec. 2020, Art. no. 118780.

[36] D. S. Pillai, N. Rajasekar, J. P. Ram, and V. K. Chinnaiyan, "Design and testing of two phase array reconfiguration procedure for maximizing power in solar PV systems under partial shade conditions (PSC)," *Energy Convers. Manag.*, vol. 178, pp. 92–110, Dec. 2018.

[37] R. D. A. Raj and K. A. Naik, "Optimal reconfiguration of PV array based on digital image encryption algorithm: A comprehensive simulation and experimental investigation," *Energy Convers. Manag.*, vol. 261, Jun. 2022, Art. no. 115666.

[38] P. R. Satpathy, R. Sharma, and S. Jena, "A shade dispersion interconnection scheme for partially shaded modules in a solar PV array network," *Energy*, vol. 139, pp. 350–365, Nov. 2017.

[39] P. R. Satpathy and R. Sharma, "Power and mismatch losses mitigation by a fixed electrical reconfiguration technique for partially shaded photovoltaic arrays," *Energy Convers. Manag.*, vol. 192, pp. 52–70, Jul. 2019.

[40] R. D. A. Raj and K. A. Naik, "A generalized Henon map-based solar PV array reconfiguration technique for power augmentation and mismatch mitigation," *IETE J. Res.*, pp. 1–19, Mar. 2022.

PRADYUMNA MALLICK received the B.Tech. degree in electrical engineering and the M.Tech. degree in power system engineering, in 2012 and 2015, respectively. He is currently pursuing the Ph.D. degree with Siksha 'O' Anusandhan Deemed to be University, Bhubaneswar, India. He is also a part-time Research Scholar with Siksha 'O' Anusandhan Deemed to be University. He is an Assistant Professor with the Rajdhani Engineering College, Bhubaneswar. His research interests include solar PV systems, microgrid, and smart grids.

RENU SHARMA (Senior Member, IEEE) received the master's degree in electrical engineering from Jadavpur University, in 2006, and the Ph.D. degree in electrical engineering from Siksha 'O 'Anusandhan Deemed to be University, Bhubaneswar, India, in 2014. She has around 20 years of leading impactful technical, professional, and educational experience. Currently, she is a Professor and the Head of the Department of Electrical Engineering, SOA Deemed to be University. She has published around 80 international journals and conference papers. Her research interests include smart grids, soft computing, solar photovoltaic systems, power system scheduling, evolutionary algorithms, and wireless sensor networks. She is a Life Member of IE (India), ISTE, and ISSE; a member of IET; and the Chair of WIE IEEE Bhubaneswar Sub Section. She was the General Chair of IEEE ODICON 2021, flagship conference IEEE WIECON-ECE 2020, and Springer conference GTSCS-2020 and IEPCCT-2019. She is a Guest Editor of Special Issue in *International Journal of Power Electronics* and *International Journal of Innovative Computing and Applications* and *Inderscience*.

PRIYA RANJAN SATPATHY received the Ph.D. degree in solar photovoltaic power system (electrical engineering) from Siksha 'O' Anusandhan Deemed to be University, India, under fellowship by CSIR, Government of India, in 2022. He is currently a Research Associate with the Department of Electrical and Electronics Engineering (EEE), Chaitanya Bharati Institute of Technology (CBIT), Hyderabad, India, under a project supported by Najran University, Saudi Arabia. He was with the Council of Scientific and Industrial Research (CSIR), as a Senior Research Fellow, from 2021 to 2022. He has depth knowledge on different PV system software, including PVSyst, PVSOL, Sketchup, Helioscope, and AutoCAD. He has published two Indian patents and more than 40 international journals and conferences. His research interests include solar power systems, PV array efficiency improvement and fault reduction, maximum power point tracking, and PV system design and installation (off-grid and on-grid). He has reviewed more than 150 papers till date. He has been serving as an Associate Editor for Taylor and Francis and a Reviewer for many international conferences and journals, such as IEEE, Elsevier, IET, Wiley, Springer, Frontiers, Taylor and Francis, and Hindawi.

SUDHAKAR BABU THANIKANTI (Senior Member, IEEE) received the B.Tech. degree from Jawaharlal Nehru Technological University, Ananthapur, India, in 2009, the M.Tech. degree in power electronics and industrial drives from Anna University, Chennai, India, in 2011, and the Ph.D. degree from VIT University, Vellore, India, in 2017. He has completed Postdoctoral Research Fellowship with the Department of Electrical Power Engineering, Institute of Power Engineering, University Tenaga Nasional (UNITEN), Malaysia. He was with the Department of Electrical and Electronic Engineering Science, University of Johannesburg, as a Senior Research Associate. Currently, he is an Associate Professor with the Department of Electrical and Electronics Engineering, Chaitanya Bharati Institute of Technology, Hyderabad. He has published more than 140 research articles in various renowned international journals. His research interests include design and implementation of solar PV systems, renewable energy resources, power management for hybrid energy systems, storage systems, fuel cell technologies, electric vehicle, and smart grids. He has been acting as an Editorial Board Member and a Reviewer of various reputed journals, such as the IEEE, IEEE Access, IET, Elsevier, and Taylor and Francis.

NNAMDI I. NWULU (Senior Member, IEEE) is currently a Full Professor with the Department of Electrical and Electronic Engineering Science, University of Johannesburg, and the Director of the Centre for Cyber Physical Food, Energy and Water Systems (CCP-FEWS). His research interests include the application of digital technologies, mathematical optimization techniques, and machine learning algorithms in food, energy, and water systems. He is a Professional Engineer registered with the Engineering Council of South Africa (ECSA), a Senior Member of the South African Institute of Electrical Engineers (SMSAIEE), and a Y-Rated Researcher by the National Research Foundation of South Africa. He is the Editor-in-Chief of the *Journal of Digital Food Energy and Water Systems* (JDFEWS) and an Associate Editor of *IET Renewable Power Generation* (IET-RPG) and *African Journal of Science, Technology, Innovation and Development* (AJSTID).

• • •